Cell

Bleach Activates a Redox-Regulated Chaperone by Oxidative Protein Unfolding

J. Winter,[1,3,4] M. Ilbert,[1,3] P.C.F. Graf,[1,2,5] D. Özcelik,[1] and U. Jakob[1,2,*]
[1]Department of Molecular, Cellular, and Developmental Biology
[2]Program in Cellular and Molecular Biology
University of Michigan, Ann Arbor, MI 48109, USA
[3]These authors contributed equally to this work
[4]Present address: Institut für Biotechnologie, Department Chemie, Technische Universität München, Garching, Germany
[5]Present address: Infectious Diseases Directorate, Naval Medical Research Center, Silver Spring, MD 20910-7500, USA
*Correspondence: ujakob@umich.edu
DOI 10.1016/j.cell.2008.09.024

SUMMARY

Hypochlorous acid (HOCl), the active ingredient in household bleach, is an effective antimicrobial produced by the mammalian host defense to kill invading microorganisms. Despite the widespread use of HOCl, surprisingly little is known about its mode of action. In this study, we demonstrate that low molar ratios of HOCl to protein cause oxidative protein unfolding in vitro and target thermolabile proteins for irreversible aggregation in vivo. As a defense mechanism, bacteria use the redox-regulated chaperone Hsp33, which responds to bleach treatment with the reversible oxidative unfolding of its C-terminal redox switch domain. HOCl-mediated unfolding turns inactive Hsp33 into a highly active chaperone holdase, which protects essential *Escherichia coli* proteins against HOCl-induced aggregation and increases bacterial HOCl resistance. Our results substantially improve our molecular understanding about HOCl's functional mechanism. They suggest that the antimicrobial effects of bleach are largely based on HOCl's ability to cause aggregation of essential bacterial proteins.

INTRODUCTION

The accumulation of reactive oxygen species (ROS), a condition termed oxidative stress, is associated with a variety of different human diseases (Aliev et al., 2002). ROS also serve beneficial roles for mammals during host defense, when macrophages and neutrophils produce high concentrations of hydrogen peroxide (H_2O_2), superoxide (O_2^-), and hypochlorous acid (HOCl) to kill invading microorganisms (Miller and Britigan, 1997).

The heat shock protein Hsp33 is a member of a highly conserved family of molecular chaperones that specifically protects bacteria against the lethal consequences of oxidative stress at elevated temperatures (i.e., oxidative heat stress) (Winter et al., 2005). Recent in vitro studies confirmed that Hsp33 utilizes a dual stress-sensing mechanism that responds to the simultaneous presence of oxidants (e.g., H_2O_2) and mild protein unfolding conditions (e.g., elevated temperatures or 1 M guanidinium-hydrochloride) with the activation of its chaperone function (Ilbert et al., 2007). H_2O_2-sensing occurs through a four-cysteine zinc center, while elevated temperatures are sensed by an adjacent linker region whose conformation appears to control the reactivity or accessibility of two of Hsp33's four redox-active cysteines, Cys^{232} and Cys^{234} (Ilbert et al., 2007; Leichert et al., 2008). Exposure of Hsp33 to oxidative heat stress leads to the consecutive formation of both intramolecular disulfide bonds and zinc(II) release (Graumann et al., 2001). These posttranslational modifications cause Hsp33's linker region and zinc-binding domain to adopt a natively unfolded structure (Graf et al., 2004; Ilbert et al., 2007). Large hydrophobic surfaces, which are the likely binding sites for unfolded proteins, become exposed, and Hsp33 assembles into the dimeric, fully active chaperone (Graf et al., 2004; Ilbert et al., 2007).

Hsp33's activation requires both peroxide stress and heat stress, whereas neither peroxide treatment alone nor high temperatures alone causes the activation of Hsp33 either in vitro or in vivo (Ilbert et al., 2007; Winter et al., 2005). This makes good physiological sense; peroxide stress itself does not cause protein unfolding in vivo and therefore does not require additional chaperones (Ilbert et al., 2007), whereas protein unfolding induced by elevated temperatures is effectively prevented by ATP-dependent chaperones, such as the DnaK-system (Mayer et al., 2001). Oxidative heat stress, however, causes protein unfolding and simultaneously decreases cellular ATP levels, which incapacitates ATP-dependent chaperones (Winter et al., 2005). Activation of Hsp33's ATP-independent chaperone function under these specific stress conditions appears therefore to compensate for the functional loss of ATP-dependent chaperones.

These findings helped explain the cytoprotective effects of Hsp33 under oxidative heat stress conditions. However, these results also raised the questions as to when and how often organisms encounter conditions that cause oxidative stress conditions that lead to protein unfolding in nature. In this study, we identified HOCl, the active ingredient of household bleach, as a reagent that rapidly induces oxidative protein unfolding in vitro and causes irreversible protein aggregation in vivo. This capacity likely contributes to the highly bactericidal effect of

Leading Edge
Review

Cell

Polarity and Differential Inheritance—Universal Attributes of Life?

Ian G. Macara[1,*] and Stavroula Mili[1]
[1]Department of Microbiology, Center for Cell Signaling, University of Virginia School of Medicine, Charlottesville, VA 22908-0577, USA
*Correspondence: igm9c@virginia.edu
DOI 10.1016/j.cell.2008.11.006

When and why did cell polarization arise? Recent work in bacteria and yeast suggests that polarization may have evolved to restrict senescence to one daughter during division by enabling the differential segregation of damaged material. In more complex organisms, polarity functions have diversified to permit the differential inheritance of centrosomes, RNAs, proteins, and membranes, which is essential for the generation of diverse cell types from stem cells and for morphogenesis.

Aging and the Origins of Cell Polarity

What do we mean by cell polarity? And how and why did it evolve? In broad terms, polarization implies the existence in any object not just of asymmetry but also of directionality. Actin microfilaments, for example, are polarized, whereas intermediate filaments and septin filaments are not, although all of these structures are asymmetric in the sense that they have a long and short axis. Applied to cells, the idea of directionality distinguishes morphologically unpolarized organisms from those that possess a clear polarity. This is most easily seen in unicellular organisms. For example, *Staphylococcus aureus* is spherical, whereas the bacterium *Escherichia coli* and the fission yeast *Schizosaccharomyces pombe* are asymmetric in the sense that their cell shapes are cylindrical, but the two poles of the cylinder appear to be identical. Morphologically, therefore, they are unpolarized. On the other hand, *Vibrio cholerae* and *Caulobacter crescentum* provide instances of prokaryotes that are highly polarized: each has a flagellum at only one pole (Figure 1A).

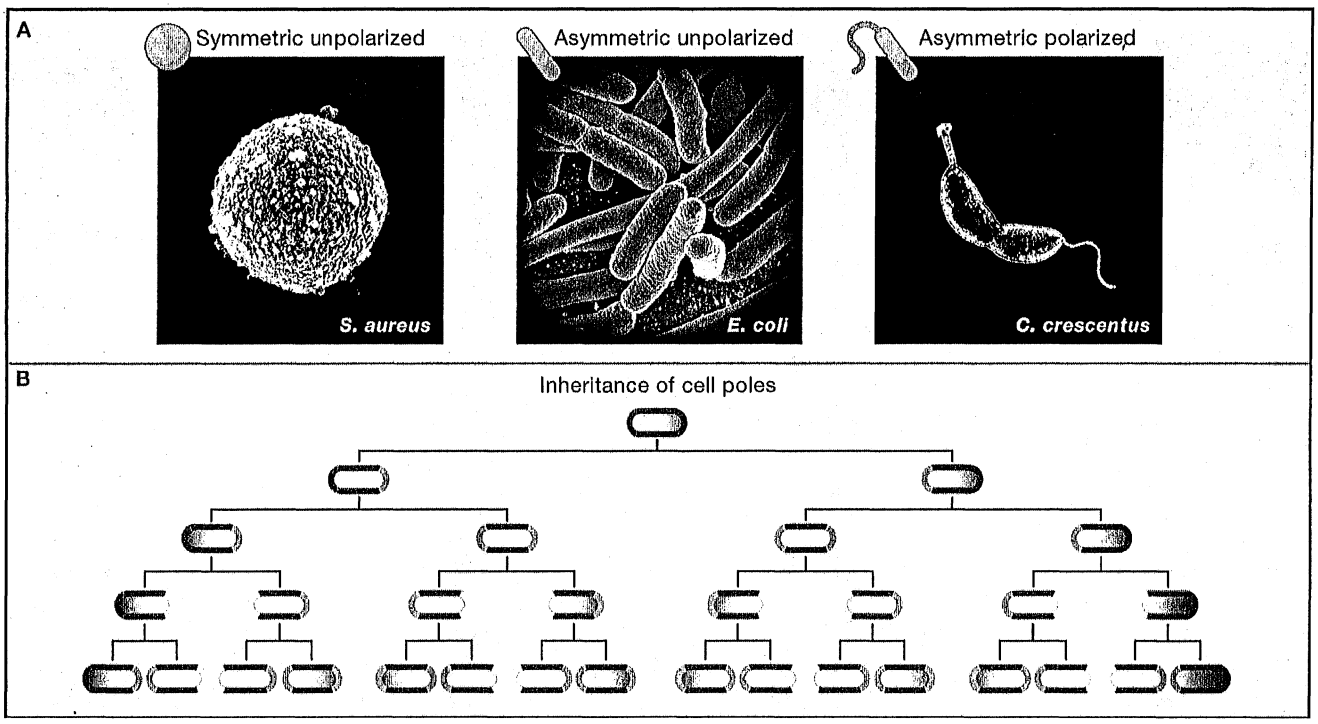

Figure 1. Types of Cell Polarity
(A) Degrees of cell polarization, with examples. (Electron micrograph of *Staphylococcus aureus* courtesy of T. Bae and O. Schneewind, University of Chicago; image of *Caulobacter crescentus* by Y. Brun, University of Indiana; electron micrograph of *Escherichia coli*, Rocky Mountain Laboratories, National Institute of Allergy and Infectious Diseases, National Institutes of Health.)
(B) Inheritance of old poles by a symmetrically dividing cell, such as *E. coli*. The oldest pole is purple. One cell will always retain this pole, whereas the other pole will always be new. If proteins or other cellular components can recognize old from new poles (gray), they can be segregated asymmetrically during each cell division.

Leading Edge
Essay

Cell

Microscopes for Fluorimeters: The Era of Single Molecule Measurements

Ronald D. Vale[1,*]
[1]Department of Cellular and Molecular Pharmacology and the Howard Hughes Medical Institute, University of California, San Francisco, San Francisco, CA 94143, USA
*Correspondence: vale@cmp.ucsf.edu
DOI 10.1016/j.cell.2008.11.009

As transforming as the first atomic resolution view of myoglobin in the late 1950s, scientists can now use a suite of single molecule technologies to watch protein macromolecular machines executing their functions "in real time." This Essay highlights applications and challenges of single molecule studies in structural biology, cell biology, and biotechnology.

Valuable information is often lost when data from a large population are examined in aggregate. To illustrate this, let us consider the recent and historic presidential election, where the popular vote favored Barack Obama (53%) over John McCain (46%). These numbers convey the outcome, but little more. However, progressively greater insight into American sociology and culture can be derived from the voting records of each of the 50 states, from individual counties within these states, and finally from exit polls of individual voters.

In biology, measurements of individuals also can reveal new information that would otherwise be lost in ensemble averages. Biochemists and biophysicists have traditionally used fluorimeters or spectrophotometers in their trade, which at best detect the activity of 50 million proteins (~a femptomole). However, many are now turning toward microscopes that can measure outputs from single molecules. In addition to enabling researchers to study vanishingly small amounts of material, single molecule technologies permit analysis of heterogeneous molecular populations or complex kinetics and dynamics of chemically identical molecules. Furthermore, single molecule measurements have allowed the study of protein outputs that previously were very difficult to explore (e.g., forces and steps of molecular motors). Applying a similar logic on a larger scale, cell biologists are uncovering new information about how cells make decisions and integrate information from their environment by measuring outputs from individual cells.

The broad impact of single molecule technologies also illustrates how rapid advances can be made through physicists, biologists, and chemists working together to solve important problems in the biological sciences. Physicists and biophysicists have contributed by developing new microscopes that can measure outputs of single molecules with stunning accuracy. Biologists and chemists have participated in this partnership by engineering molecules and developing fluorescent dyes for single molecule assays. As pioneers continue to push the limits of what can be measured at the single molecule level, they have left behind a "wake" of mature and readily accessible technologies and methods. Indeed, many single molecule measurements have become relatively easy to perform. One goal of this Essay is to encourage more laboratories to incorporate these techniques into their routine toolkit for studying macromolecules both in vitro and in vivo.

A Historical Perspective

A brief history of single molecule measurements in biology illuminates the trajectory of the field and the diverse methodologies that have emerged. The development of patch clamp recordings by Neher and Sakmann in 1976 represented the birth of single molecule measurements. This revolutionary technique, capable of measuring the 10^{-12} amps of current flowing through a single ion channel, enabled researchers to measure individual opening and closing events, reflecting the underlying conformational changes in the pore of the ion channel. Despite the enormous benefit of patch clamp measurements to neurophysiology and the biophysical understanding of ion channels (and awarding of the Nobel Prize to Neher and Sakmann in 1991), it took many years before single molecule measurements spread to other biological disciplines. Perhaps ion channels were viewed as a "special case," given that the signal (current) from a single molecule could be greatly amplified. However, outputs of single molecules can be measured with clever assays that do not require sophisticated technologies. Probably more likely, biochemists in the 1970s and 1980s did not yet envisage a compelling reason to invest their energies in making single molecule measurements. The spectrofluorimeter still ruled the kingdom.

One of the first "single molecule" experiments to follow ion channels was the measurement of individual microtubules (Mitchison and Kirschner, 1984). The polymerization of tubulin into cylindrical 25 nm diameter microtubules was routinely measured by detecting the scattered light using a spectrophotometer. When the polymerization reaction reached a steady state (polymer mass remaining constant), little change in microtubule length was expected, as the rates of subunit addition and dissociation should be equal. By looking at individual microtubules by immunofluorescence and measuring their length at steady state, Mitchison and Kirschner discovered surprisingly that some of the microtubules in the population were growing

Cell

Green Fluorescent Protein Glows Gold

Atsushi Miyawaki[1,2,*]
[1]Laboratory of Cell Function and Dynamics, Riken Brain Science Institute
[2]Life Function and Dynamics, ERATO, Japan Science and Technology Agency
Saitama, 351-0198 Japan
*Correspondence: matsushi@brain.riken.jp
DOI 10.1016/j.cell.2008.11.025

The awarding of this year's Nobel Prize in Chemistry to Osamu Shimomura, Martin Chalfie, and Roger Tsien for their discovery and development of green fluorescent protein earns this humble jellyfish protein a place of honor in the biology research hall of fame.

This year, the Royal Swedish Academy of Sciences has awarded the Nobel Prize in Chemistry jointly to Osamu Shimomura of the Woods Hole Marine Biological Laboratory, Martin Chalfie of Columbia University, and Roger Y. Tsien of the University of California, San Diego (Figure 1). The Prize has been awarded for their discovery and development of green fluorescent protein (GFP)—first identified in the jellyfish *Aequorea victoria*—that has become one of the most important tools used in contemporary biology research. Although many molecules involved in biological systems have been identified and the hierarchy among these molecules has been elucidated, further understanding will require knowledge of how each component of the system is controlled in space and time. In the post-genomics era, researchers need a tool that enables the direct visualization of biological functions, and GFP has turned out to be that tool.

GFP has a particularly unique history and one that has benefitted from the work of each of the three Nobel Laureates. From the discovery of the protein itself by Osamu Shimomura and the first expression studies by Martin Chalfie to the development of GFP and its many variants as ubiquitous laboratory tools by Roger Y. Tsien, it is both instructive and inspirational to review the life experiences and achievements of these three remarkable scientists.

Discovery

In 1961, newly arrived from Nagoya University, Japan, Osamu Shimomura began studying bioluminescence in the jellyfish *Aequorea victoria* with Frank H. Johnson at the University of Washington's Friday Harbor Laboratory, located on a small island near Victoria, British Columbia, Canada (Figure 2). The jellyfish displays a bright ring of green luminescence along the edge of its umbrella upon chemical or mechanical stimulation (Figure 2, inset). Every summer, from 1961 through the early 1990s, huge numbers of *Aequorea victoria* were skimmed from the sea by Friday Harbor researchers wielding long-handled nets. Initially, the precious jellyfish umbrella margins were removed with scissors; later on, harvesters adopted a specialized device (Figure 2) called a "jellyfish cutter." By the early 21st century, the species was virtually absent locally from the pelagic ecosystem, although this is probably due to environmental changes rather than zealous overcollection by eager scientists.

In the 1960s, Shimomura identified and characterized the luminescent and fluorescent molecules responsible for *Aequorea*'s bioluminescence (Shimomura, 1998). The luminescent molecule is the calcium-binding protein aequorin, which produces blue light in the pres-

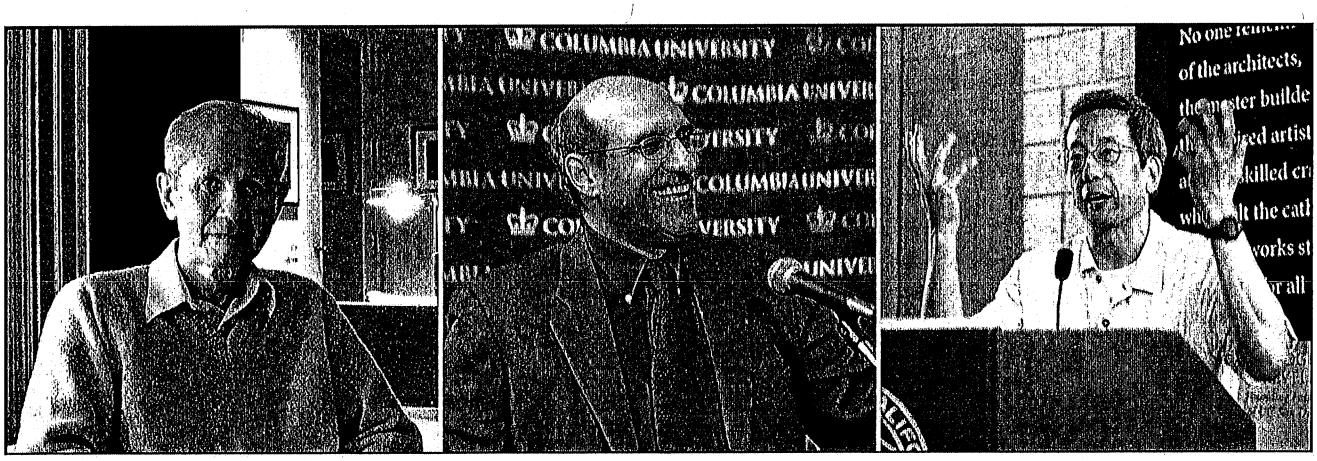

Figure 1. Everything Is Illuminated
This year's Nobel Laureates in Chemistry are (left) Osamu Shimomura of the Woods Hole Marine Biological Laboratory, (middle) Martin Chalfie of Columbia University, and (right) Roger Y. Tsien of the University of California, San Diego. (Images courtesy of A. Miyawaki, Columbia University press office, and UCSD press office.)

The EMBO Journal (2008) 27, 3081–3091 | © 2008 European Molecular Biology Organization | All Rights Reserved 0261-4189/08
www.embojournal.org

THE EMBO JOURNAL

Determination of bacterial rod shape by a novel cytoskeletal membrane protein

Daisuke Shiomi[1], Masako Sakai[1] and Hironori Niki[1,2,*]

[1]Microbial Genetics Laboratory, Genetic Strains Research Center, National Institute of Genetics, Mishima, Japan and [2]Department of Genetics, The Graduate University for Advanced Studies, Mishima (SOKENDAI), Shizuoka, Japan

Cell shape is critical for growth, and some genes are involved in bacterial cell morphogenesis. Here, we report a novel gene, *rodZ*, required for the determination of rod shape in *Escherichia coli*. Cells lacking *rodZ* no longer had rod shape but rather were round or oval. These round cells were smaller than known round mutant cells, including *mreB* and *pbpA* mutants; both are known to lose rod shape. Morphogenesis from rod cells to round cells and *vice versa*, caused by depletion and overproduction of RodZ, respectively, revealed that RodZ could regulate the length of the long axis of the cell. RodZ is a membrane protein with bitopic topology such that the N-terminal region including a helix-turn-helix motif is in the cytoplasm, whereas the C-terminal region is exposed in the periplasm. GFP–RodZ forms spirals along the lateral axis of the cell beneath the cell membrane, similar to the MreB bacterial actin. Thus, RodZ may mediate spatial information from cytoskeletal proteins in the cytoplasm to a peptidoglycan synthesis machinery in the periplasm.

The EMBO Journal (2008) **27**, 3081–3091. doi:10.1038/emboj.2008.234; Published online 13 November 2008
Subject Categories: cell & tissue architecture; microbiology & pathogens
Keywords: cytoskeleton; morphology; peptidoglycan; RodZ; spherical cell

Introduction

Bacteria display a variety of cell shapes, including round, rod, spiral, and amorphous (Young, 2006). Maintenance of cell shape is vital for cell growth and cell division in most bacteria. The distinct shape of most bacteria is retained by a peptidoglycan layer, or sacculus, enveloping bacterial cells because the sacculus is a single giant macromolecule (Vollmer and Bertsche, 2008). The sacculus serves as a rigid body against mechanical stress, including osmotic pressure of the cytoplasm. In fact, inactivation of peptidoglycan synthesis by some antibiotics causes the cells to burst by osmotic pressure, leading to cell death. Gram-positive *Bacillus subtilis* and Gram-negative *Escherichia coli* bacteria are enveloped in the peptidoglycan layer made of glycan strands cross-linked by short peptides in different manners. Obviously, the peptidoglycan layer of Gram-positive bacteria is thicker than that of Gram-negative bacteria.

Morphogenesis of the peptidoglycan layer is regulated not only by peptidoglycan biosynthesis, but also by cytoskeletal proteins beneath the cytoplasmic membrane (Osborn and Rothfield, 2007). It has been shown that most bacteria have homologues of eukaryotic cytoskeletal proteins, such as tubulin and actin (Carballido-Lopez and Formstone, 2007; Dye and Shapiro, 2007; Erickson, 2007; Graumann, 2007; Osborn and Rothfield, 2007; Pichoff and Lutkenhaus, 2007). The bacterial tubulin, FtsZ, has an important function in cell division (Margolin, 2005) and contributes to cell morphogenesis. FtsZ forms a ring-like structure at mid-cell, which serves as a scaffold for other cell division proteins. The other bacterial cytoskeletal protein is actin homologue MreB. MreB has been originally identified from a mutant showing aberrant cell morphogenesis in *E. coli* (Wachi *et al*, 1987). *mreB* is conserved in a wide range of bacterial species, and it has been shown that MreB in *B. subtilis* has a cytoskeletal function in bacterial cell morphogenesis (Jones *et al*, 2001), and this finding has opened the door to research on the regulation of cell morphology through cytoskeletal proteins. In addition to MreB, *B. subtilis* has two other MreB paralogues, Mbl and MreBH (Jones *et al*, 2001; Carballido-Lopez *et al*, 2006), and at least two of the three MreB paralogues seem to be required to maintain the rod shape. MreB determines the length of the short axis of the cell, whereas Mbl determines the length of the long axis of the cell (Jones *et al*, 2001). It is reported that MreB mutants affect the length of the short axis of the *E. coli* cells (Kruse *et al*, 2003). Moreover, Mbl has been shown to be required for helical insertion of peptidoglycan (Daniel and Errington, 2003). Both MreB and Mbl form a helix or filament just beneath the cytoplasmic membrane along the long axis of the cell in *B. subtilis* (Jones *et al*, 2001).

Penicillin-binding proteins (PBPs), including PBP2, are enzymes involved in peptidoglycan metabolism. Some of the PBPs and enzymes required for synthesis of the peptidoglycan layer have been shown to interact with the multicomplex, including MreB, MreC, and MreD (Divakaruni *et al*, 2005, 2007; van den Ent *et al*, 2006; Mohammadi *et al*, 2007). The absence of these components of the complex results in abnormal cell shapes, such as round or Y shape, because the cells cannot synthesize the peptidoglycan layer and divide correctly (Young, 2003); these cells eventually die (Bendezu and de Boer, 2008). It is known that MreB and PBP2 serve to maintain the length of the short axis in *E. coli* (Den Blaauwen *et al*, 2003; Kruse *et al*, 2003). In fact, both MreB and PBP2 seem to have important functions in synthesis of the peptidoglycan layer in *E. coli* (Uehara and Park, 2008). A variety of proteins, including PBPs, bacterial actin homologues (MreB, Mbl, and MreBH), and their interaction partners (RodA,

*Corresponding author. Microbial Genetics Laboratory, Genetic Strain Research Center, National Institute of Genetics, 1111 Yata, Mishima, Shizuoka 411-8540, Japan. Tel.: +81 55 981 6870; Fax: +81 55 981 6826; E-mail: hniki@lab.nig.ac.jp

Received: 29 August 2008; accepted: 15 October 2008; published online: 13 November 2008

Fission yeast Ccq1 is telomerase recruiter and local checkpoint controller

Kazunori Tomita and Julia Promisel Cooper[1]

Telomere Biology Laboratory, Cancer Research UK, London WC2A 3PX, United Kingdom

Telomeres recruit telomerase and differentiate chromosome ends from sites of DNA damage. Although the DNA damage checkpoint PI3-kinases ATM and ATR localize to telomeres and promote telomerase activation, activation of their downstream checkpoint pathway targets is inhibited. Here, we show that the fission yeast telomeric protein Ccq1 is required for telomerase recruitment and inhibition of ATR target activation at telomeres. The loss of Ccq1 results in progressive telomere shortening and persistent ATR-dependent activation of Chk1. Unlike the checkpoint activation that follows loss of telomerase, this checkpoint activation occurs prior to detectable levels of critically short telomeres. When *ccq1Δ* telomeres do become critically short, activated Chk1 promotes an unusual homologous recombination-based telomere maintenance process. We find that the previously reported meiotic segregation defects of cells lacking Ccq1 stem from its role in telomere maintenance rather than from a role in formation of the meiotic bouquet. These findings demonstrate the existence of a novel telomerase recruitment factor that also serves to suppress local checkpoint activation.

[*Keywords*: Telomere; telomerase; DNA damage checkpoint; homologous recombination; mitosis; meiosis]

Supplemental material is available at http://www.genesdev.org.

Received July 25, 2008; revised version accepted October 31, 2008.

The telomeric repeats that comprise terminal chromosomal DNA assemble protein complexes that differentiate bona fide chromosomal ends from damaged DNA. Hence, telomeres prevent chromosome ends from eliciting their own fusion and recombination, and from triggering checkpoint-induced cell cycle arrest. Nonetheless, numerous DNA damage response proteins, including MRN (the Mre11–Rad50–Nbs1 complex), Ku, ATM, and ATR, localize to telomeres and play important roles in normal telomere metabolism (Gravel et al. 1998; Zhu et al. 2000; Nakamura et al. 2002; Takata et al. 2005; Verdun and Karlseder 2006). How telomeres prevent these factors from inappropriately responding to chromosome ends is one of the persisting mysteries of chromosome biology.

Telomeric DNA is degraded every cell cycle in a replication-associated manner. Critically short telomeres lose the ability to protect chromosome ends from being recognized as DNA damage. Accordingly, short telomeres elicit the cell cycle arrest pathways that robust telomeres inhibit, leading to cellular senescence or apoptosis. In order to maintain proliferation, germ cells, cancer cells, and unicellular organisms employ the telomere-specific reverse transcriptase, telomerase, to replenish terminal telomere repeats. Telomerase activity can be reconstituted in vitro from only two essential components, the catalytic protein subunit of the reverse transcriptase and the telomeric RNA template (Lingner et al. 1997). However, in vivo telomerase activity requires several additional subunits that mediate the recruitment and activation of telomerase in a telomere attrition- and cell cycle-dependent manner (Taggart et al. 2002; Teixeira et al. 2004; Bianchi and Shore 2007; Sabourin et al. 2007). Regulation of telomerase activity is so far best understood in budding yeast. Recruitment of Est2 (the catalytic subunit) to short telomeres in late S phase is mediated by the telomerase-binding protein Est1, which in turn associates with TLC1 (the telomerase RNA) and the single-stranded telomeric DNA-binding protein Cdc13 (Singer and Gottschling 1994; Lin and Zakian 1995; Lendvay et al. 1996; Nugent et al. 1996; Evans and Lundblad 1999; Qi and Zakian 2000; Taggart et al. 2002; Bianchi et al. 2004; Sabourin et al. 2007); modification of one or more telomere components by ATM/ATR confers at least part of the telomere attrition and cell cycle dependence of telomerase activation (Takata et al. 2005; Tseng et al. 2006). In fission yeast, the telomerase complex contains Trt1 (the Est2 homolog), the RNA template Ter1, and Est1 (Nakamura et al. 1997; Beernink et al. 2003; Leonardi et al. 2008; Webb and Zakian 2008). In addition, telomere maintenance requires the telomere single-strand-binding protein Pot1 (Baumann and Cech 2001). The Pot1 complex has recently been purified and found to contain three additional proteins—Tpz1, Poz1, and Ccq1 (see below) (Mi-

[1]Corresponding author.
E-MAIL Julie.cooper@cancer.org.uk; FAX 44-0207-2693258.
Article is online at http://www.genesdev.org/cgi/doi/10.1101/gad.498608.

J|A|C|S
COMMUNICATIONS

Published on Web 11/24/2008

Superresolution Microscopy on the Basis of Engineered Dark States

Christian Steinhauer, Carsten Forthmann, Jan Vogelsang, and Philip Tinnefeld*

Angewandte Physik – Biophysik, and Center for NanoScience, Ludwig-Maximilians-Universität, Amalienstrasse 54, 80799 München, Germany

Received August 19, 2008; E-mail: Philip.Tinnefeld@lmu.de

Recent advances in fluorescence microscopy have broadened our imagination of what is possible using far-field fluorescence microscopy. New concepts such as stimulated emission depletion (STED) microscopy and subdiffraction resolution imaging by subsequent localization of single molecules (i.e. concepts denoted STORM, dSTORM, PALM, FPALM, etc.) are rapidly emerging and provide new ways to resolve structures beyond the 200 nm scale.[1−9] Due to their conceptual and technical simplicity, the latter techniques based on wide-field imaging of single fluorophores have spread enormously. Yet, a severe disadvantage of these techniques is that they rely on photoactivatable or photoswitchable fluorophores limiting their general applicability and multiplexing capacity.[10−14]

The common principle of subdiffraction resolution microscopy by subsequent single-molecule localizations is that only one point-like light source is active for a diffraction limited area at any time. This fluorophore is localized by imaging with a sensitive camera. In the beginning of data acquisition all except a few fluorophores are prepared in the off-state and the number of active fluorophores is kept constant by applying an activating light source that compensates for the loss of fluorophores by photobleaching or switching off. Instead of stroboscopic alternating illumination to prepare the desired number of molecules in the on-state and then read-out and switch-off again, more recent schemes apply simultaneous excitation with both the read-out/switch-off wavelengths and the activating wavelength.[7,15] Here the intensities of the lasers are adapted to balance the rate of switching molecules on and off.

In this communication, we engineer on- and off-states by controlling the photophysics of the fluorophores by electron transfer reactions. We exploit these engineered dark states for subdiffraction resolution fluorescence microscopy of single molecules, actin filaments, and microtubules in fixed cells. This strategy is essentially applicable to all synthetic, single-molecule compatible fluorophores and not restricted to a few photoswitchable or photoactivatable derivatives, since dark states ("blinking") can be induced for every fluorophore, e.g., by increasing the triplet state lifetime through oxygen removal or by inducing radical-ion states. The key issue to using this blinking for superresolution microscopy is to localize a sufficient number of fluorophores within a diffraction limited spot. This number is directly linked to the ratio of the off-times to the on-times of the fluorophores as well as to the data acquisition speed. To be able to resolve as many fluorophores as possible in a diffraction limited spot it is the aim to have very short but bright on-states and long off-states. On the other hand controlling the off-state duration with a balance of fast acquisition and high resolution is desired.[16] To this end, the length of the off-state limits the achievable spatial resolution since due to technical limitations of the camera's acquisition speed the resolution cannot be improved infinitely by reducing on-state duration through high excitation intensities. The natural lifetime of the triplet state typically is in the lower millisecond range in the absence of oxygen and poses an upper limit of the dark state duration. We suggest using electron transfer reactions to extend the range of achievable on- and off-times.[17] With freshly dissolved ascorbic acid (AA) we can extend the off-state lifetimes of many fluorophores severalfold.

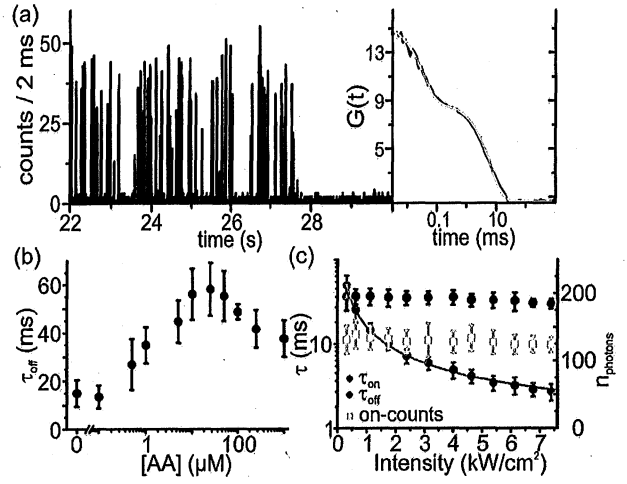

Figure 1. Controlling blinking for superresolution microscopy. (a) Part of a fluorescence transient of single Cy5 in oxygen depleted phosphate buffered saline (PBS) with ascorbic acid (AA, 100 μM, 2 ms binning). Inset shows the autocorrelation function yielding $\tau_{cis-trans} = 70\ \mu s$ and $\tau_{off} = 60$ ms. (b) Dependence of τ_{off} on AA concentration. (c) Dependence of τ_{on}, τ_{off}, and the number of photons detected per on-state (on-counts) on excitation power (c(AA) = 200 μM).

Figure 1a shows a fluorescence intensity transient of a single Cy5 labeled DNA in PBS after enzymatic removal of oxygen and addition of 100 μM AA as well as the corresponding autocorrelation function with a biexponential fit. The short fluctuation component with an off-time of 70 μs is ascribed to cis−trans isomerization,[10] and the long component of $\tau_{off} = 60$ ms is ascribed to the formation of a radical anion (assuming a neutral fluorophore).[17] In the absence of AA, the long off-state represents the triplet state with $\tau_T = (14 \pm 5)$ ms (Figure 1b). By increasing the AA concentration the lifetime of the long off-state increases up to (60 ± 8) ms since the triplet state is reduced to a radical anion (Figure 1b). At higher AA concentrations the off-states become slightly shorter likely due to an oxidizing impurity.[17]

Next we studied control of the on-state lifetime and the localization precision that can be obtained from the available counts emitted during an on-state (on-counts). The on-state lifetime is reduced by increasing the excitation intensity since dark-state formation is a photoinduced process. The on-times are reduced to ~2 ms already at moderate excitation intensities (Fig. 1c), i.e., a time typical for current CCD camera maximum acquisition speeds. The number of photons detected per-on-time remains constant at ~130 photons (Figure 1c) and is sufficient for a localization precision of single molecules of $\sim s/(n^{1/2}) = 22$ nm, where s represents the standard deviation of the point-spread-function.[18] It

10.1021/ja806590m CCC: $40.75

J|A|C|S
ARTICLES
Published on Web 11/17/2008

Photostable Single-Molecule Nanoparticle Optical Biosensors for Real-Time Sensing of Single Cytokine Molecules and Their Binding Reactions

Tao Huang, Prakash D. Nallathamby, and Xiao-Hong Nancy Xu*

Department of Chemistry and Biochemistry, Old Dominion University, Norfolk, Virginia 23529

Received August 31, 2008; E-mail: xhxu@odu.edu

Abstract: We synthesized tiny stable silver nanoparticles (2.6 ± 1.1 nm) and used its small surface area and functional groups to control single molecule detection (SMD) volumes on single nanoparticles. These new approaches allowed us to develop intrinsic single molecule nanoparticle optical biosensors (SMNOBS) for sensing and imaging of single human cytokine molecules, recombinant human tumor necrosis factor-α (TNFα), and probing its binding reaction with single monoclonal antibody (MAB) molecules in real-time. We found that SMNOBS retained their biological activity over months and showed exceptionally high photostability. Our study illustrated that smaller nanoparticles exhibited higher dependence of optical properties on surface functional groups, making it a much more sensitive biosensor. Localized surface plasmon resonance spectra (LSPRS) of SMNOBS showed a large red shift of peak wavelength of 29 ± 11 nm, as single TNFα molecules bound with single MAB molecules on single nanoparticles. Utilizing its LSPRS, we quantitatively measured its binding reaction in real time at single molecule (SM) level, showing stochastic binding kinetics of SM reactions with binding equilibrium times ranging from 30 to 120 min. SMNOBS exhibited extraordinarily high sensitivity and selectivity, and a notably wide dynamic range of 0−200 ng/mL (0−11.4 nM). Thus, SMNOBS is well suited for the fundamental study of biological functions of single protein molecules and SM interactions of chemical functional groups with the surface of nanoparticles, as well as development of effective disease diagnosis and therapy.

Introduction

Cytokines are secreted regulatory proteins and play vital roles in controlling cell survival, growth, differentiation, and function by binding with specific receptors and initiating immune regulation pathways.[1] At the cellular level, it takes only a few cytokine molecules to induce a significant cellular response,[2] underscoring the importance of developing new tools to detect and image individual cytokine molecules and to characterize their functions in real time. Tumor necrosis factor-α (TNFα), a 17.5 kDa protein, is a pro-inflammatory cytokine that can mediate a variety of biological effects, such as immune regulation, antitumor activity, viral replication, and infection resistance.[3,4] Studies have shown that a variety of pathological conditions, including cancer, heart disease, diabetes and autoimmune diseases, lead to overproduction of TNFα, and adequate doses of TNFα are vital to effectively treat diseases (e.g., cancer) without severe side effects.[3,4] Unfortunately, despite extensive research over decades, the underlying mechanisms about how TNFα mediates these crucial biological functions still remain incompletely understood and it is thus important to develop ultrasensitive assays for accurate analysis of TNFα.

Several commercially available methods have been used for detecting TNFα: enzyme-linked immunosorbent assays (ELISA),[5,6] radioimmunoassay (RIA),[7] cytotoxicity assay,[8] flow cytometry,[9] and RT-PCR.[10] The ELISA method offers high sensitivity with a detection limit of 5 pg/mL.[5,6] However, these conventional methods typically involve multiple staining and washing steps, which are time-consuming and cannot be used in quantitative analysis of TNFα in real time. Fluorescence quantum dots (QDs), protein microarray[11] and electrochemical immunoassay[12] have been developed to detect TNFα. Nanoparticle-based detection schemes and sensors have also been reported for detecting other proteins, such as prostate-specific

(1) Nicola, N. A. *Guidebook to cytokines and their receptors*; A Sambrook & Tooze Publication at Oxford University Press: Oxford, 1994, and references therein.
(2) Gurevich, K. G.; Agutter, P. S.; Wheatley, D. N. *Cell Signal* **2003**, *15*, 447–453.
(3) Tagawa, M. *Curr. Pharm. Des.* **2000**, *6*, 681–699.
(4) Haworth, C.; Maini, R. N.; Feldman, M. In *The Cytokine Handbook*; Thomson, A., Ed.; Academic Press: New York, 1998; pp 777−801.
(5) Copeland, S.; Siddiqui, J.; Remick, D. *J. Immunol. Methods* **2004**, *284*, 99–106.
(6) Klabusay, M.; Kohutova, V.; Coupek, P.; Nenickova, M.; Tesarova, E. *Mediators Inflammation* **2006**, 1–7.
(7) de Kossodo, S.; Houba, V.; Grau, G. E. *J. Immunol. Methods* **1995**, *182*, 107–114.
(8) Watts, A. D.; Onier-Cherix, N.; Hunt, N. H.; Chaudhri, G. *J. Immunol. Methods* **1999**, *225*, 179–184.
(9) Shinn, A. H.; Bravo, N. C.; Maecker, H. T.; Smith, J. W. *J. Immunol. Methods* **2003**, *282*, 169–174.
(10) Pico de Coana, Y.; Barrero, C.; Cajiao, I.; Mosquera, C.; Patarroyo, M. E.; Patarroyo, M. A. *Cytokine* **2004**, *27*, 129–133.
(11) Zajac, A.; Song, D.; Qian, W.; Zhukov, T. *Colloids Surf. B Biointerfaces* **2007**, *58*, 309–314.
(12) Wang, J.; Liu, G.; Engelhard, M. H.; Lin, Y. *Anal. Chem.* **2006**, *78*, 6974–6979.

10.1021/ja8068853 CCC: $40.75

JOURNAL OF BACTERIOLOGY, Jan. 2009, p. 231–237 Vol. 191, No. 1
0021-9193/09/$08.00+0 doi:10.1128/JB.00536-08

Cytoplasmic Protein Mobility in Osmotically Stressed *Escherichia coli*▽†

Michael C. Konopka,[1]‡ Kem A. Sochacki,[1] Benjamin P. Bratton,[1] Irina A. Shkel,[1] M. Thomas Record,[1,2] and James C. Weisshaar[1]*

Department of Chemistry, 1101 University Avenue,[1] and Department of Biochemistry,[2] University of Wisconsin—Madison, Madison, Wisconsin 53706

Received 18 April 2008/Accepted 7 October 2008

Facile diffusion of globular proteins within a cytoplasm that is dense with biopolymers is essential to normal cellular biochemical activity and growth. Remarkably, *Escherichia coli* grows in minimal medium over a wide range of external osmolalities (0.03 to 1.8 osmol). The mean cytoplasmic biopolymer volume fraction ($\langle\langle\phi\rangle\rangle$) for such adapted cells ranges from 0.16 at 0.10 osmol to 0.36 at 1.45 osmol. For cells grown at 0.28 osmol, a similar $\langle\phi\rangle$ range is obtained by plasmolysis (sudden osmotic upshift) using NaCl or sucrose as the external osmolyte, after which the only available cellular response is passive loss of cytoplasmic water. Here we measure the effective axial diffusion coefficient of green fluorescent protein (D_{GFP}) in the cytoplasm of *E. coli* cells as a function of $\langle\phi\rangle$ for both plasmolyzed and adapted cells. For plasmolyzed cells, the median D_{GFP} (D^m_{GFP}) decreases by a factor of 70 as $\langle\phi\rangle$ increases from 0.16 to 0.33. In sharp contrast, for adapted cells, D^m_{GFP} decreases only by a factor of 2.1 as $\langle\phi\rangle$ increases from 0.16 to 0.36. Clearly, GFP diffusion is not determined by $\langle\phi\rangle$ alone. By comparison with quantitative models, we show that the data cannot be explained by crowding theory. We suggest possible underlying causes of this surprising effect and further experiments that will help choose among competing hypotheses. Recovery of the ability of proteins to diffuse in the cytoplasm after plasmolysis may well be a key determinant of the time scale of the recovery of growth.

Facile diffusion of globular proteins in the cytoplasm of bacteria is essential for growth and adaptation to stress, but diffusion is hindered by the presence of other biopolymers. For *Escherichia coli* in the exponential-growth phase in minimal medium at the optimal osmolality of 0.28 osmol, 16% of the cytoplasmic volume is occupied by biopolymers (mean cytoplasmic biopolymer volume fraction [$\langle\phi\rangle$], 0.16). For growth at 1.45 osmol, $\langle\phi\rangle$ increases to about 0.36, and the growth rate decreases by a factor of 9 (4, 5). However, growth at high osmolalities can be achieved only by gradually transferring cells to growth media of successively higher osmolalities. When cells are plasmolyzed, i.e., abruptly shocked by a high external solute concentration, a substantial fraction of the cytoplasmic water is extracted on a time scale of a few seconds. Plasmolysis is the initial event that triggers subsequent osmoregulation processes: energy-dependent intake of K^+, biosynthesis of glutamate anion and neutral osmoprotectants such as trehalose, and, if plasmolysis is not too severe, eventual recovery of growth.

Proteins at high total concentrations may inhibit each other's diffusion by simple crowding (23). In addition, a substantial fraction of the biopolymer mass is part of a branched, time-varying "supermolecule" comprising the nucleoid, associated architectural proteins, RNA polymerase, nascent mRNA chains, attached ribosomes, and nascent polypeptide chains (38). The resulting cross-linked meshwork fragments free space into smaller regions interconnected by passageways that may become sufficiently narrow to hinder further protein diffusion. Such macromolecular crowding and confinement at high $\langle\phi\rangle$ values also affects the thermodynamics and kinetics of folding (33), assembly (18, 20), and binding (24). Quantitative studies of such biomolecular processes in vivo can shed new light on the remarkable ability of the cell to function over a wide range of $\langle\phi\rangle$ values (8, 14). They can also inform the kind of modeling necessary to adapt in vitro biochemical results to the living cell (6, 10).

We recently reported strong effects of increasing $\langle\phi\rangle$ on protein diffusion in vivo (17). Cytoplasmic water was extracted from a B strain of *E. coli* grown in rich medium at 0.24 osmol by plasmolysis in hyperosmotic medium lacking carbon sources and containing only membrane-impermeant solutes, either NaCl or sucrose. These conditions prohibit active K^+ uptake and the usual biochemical adaptation to osmotic stress. In effect, cells are locked into a physical and biochemical condition closely approximating the transient state that would occur immediately after a sudden osmotic upshift but before adaptation can begin. The mean effective axial diffusion coefficient ($\langle\langle D_{GFP}\rangle\rangle$) of green fluorescent protein (GFP) in the cytoplasm on a length scale of ~0.5 μm decreased by a factor of 430 as the plasmolysis osmolality increased from 0.24 to 0.94 osmol. The recovery of proteins' ability to diffuse in the plasmolyzed cytoplasm may well be a key determinant of the time scale of recovery of growth.

Here we extend the work to GFP diffusion in a K-12 strain grown in minimal medium under conditions for which the amounts of cytoplasmic water, small solutes, and biopolymers are known (4). This enables us to compare GFP diffusion in cells that have the same large value of $\langle\phi\rangle$, achieved in two very different ways: (i) growth at the optimal 0.28 osmol followed by plasmolysis and (ii) adaptation and growth at a high external

* Corresponding author. Mailing address: Department of Chemistry, 1101 University Ave., Madison, WI 53706. Phone: (608) 262-0266. Fax: (608) 262-0453. E-mail: weisshaar@chem.wisc.edu.

† Supplemental material for this article may be found at http://jb.asm.org/.

‡ Present address: Department of Chemical Engineering, University of Washington, Box 355014, Seattle, WA 98195-5014.

▽ Published ahead of print on 24 October 2008.

JOURNAL OF BACTERIOLOGY, Jan. 2009, p. 347–354 Vol. 191, No. 1
0021-9193/09/$08.00+0 doi:10.1128/JB.01238-08

Complete Genome Sequence and Comparative Genome Analysis of Enteropathogenic *Escherichia coli* O127:H6 Strain E2348/69▽†

Atsushi Iguchi,[1] Nicholas R. Thomson,[2] Yoshitoshi Ogura,[1,3] David Saunders,[2] Tadasuke Ooka,[3] Ian R. Henderson,[4] David Harris,[2] M. Asadulghani,[1] Ken Kurokawa,[5] Paul Dean,[6] Brendan Kenny,[6] Michael A. Quail,[2] Scott Thurston,[2] Gordon Dougan,[2] Tetsuya Hayashi,[1,3] Julian Parkhill,[2] and Gad Frankel[7]*

Division of Bioenvironmental Science, Frontier Science Research Center,[1] and Division of Microbiology, Department of Infectious Diseases, Faculty of Medicine,[3] University of Miyazaki, Miyazaki, Japan; Pathogen Genomics, The Wellcome Trust Sanger Institute, Wellcome Trust Genome Campus, Hinxton, Cambridge, United Kingdom[2]; School of Immunity and Infection, University of Birmingham, Birmingham, United Kingdom[4]; Department of Biological Information, School and Graduate School of Bioscience and Biotechnology, Tokyo Institute of Technology, Kanagawa, Japan[5]; Institute of Cell and Molecular Biosciences, University of Newcastle, Newcastle upon Tyne, United Kingdom[6]; and Centre for Molecular Microbiology and Infection, Division of Cell and Molecular Biology, Imperial College London, London, United Kingdom[7]

Received 5 September 2008/Accepted 15 October 2008

Enteropathogenic *Escherichia coli* (EPEC) was the first pathovar of *E. coli* to be implicated in human disease; however, no EPEC strain has been fully sequenced until now. Strain E2348/69 (serotype O127:H6 belonging to *E. coli* phylogroup B2) has been used worldwide as a prototype strain to study EPEC biology, genetics, and virulence. Studies of E2348/69 led to the discovery of the locus of enterocyte effacement-encoded type III secretion system (T3SS) and its cognate effectors, which play a vital role in attaching and effacing lesion formation on gut epithelial cells. In this study, we determined the complete genomic sequence of E2348/69 and performed genomic comparisons with other important *E. coli* strains. We identified 424 E2348/69-specific genes, most of which are carried on mobile genetic elements, and a number of genetic traits specifically conserved in phylogroup B2 strains irrespective of their pathotypes, including the absence of the ETT2-related T3SS, which is present in *E. coli* strains belonging to all other phylogroups. The genome analysis revealed the entire gene repertoire related to E2348/69 virulence. Interestingly, E2348/69 contains only 21 intact T3SS effector genes, all of which are carried on prophages and integrative elements, compared to over 50 effector genes in enterohemorrhagic *E. coli* O157. As E2348/69 is the most-studied pathogenic *E. coli* strain, this study provides a genomic context for the vast amount of existing experimental data. The unexpected simplicity of the E2348/69 T3SS provides the first opportunity to fully dissect the entire virulence strategy of attaching and effacing pathogens in the genomic context.

Escherichia coli is important because it is biology's premier model organism, is a common commensal of the vertebrate gut, and is a versatile pathogen of humans and animals. Molecular epidemiological studies have classified *E. coli* strains into a number of phylogroups (phylogroups A, B1, B2, D, and E) (13, 42), which are estimated to have diverged in the last 5 to 9 million years (37, 42). Commensal *E. coli* strains are beneficial to the host and rarely cause disease. However, several clones of *E. coli* are responsible for a spectrum of diseases, including urinary tract infection, sepsis/meningitis, and diarrhea (for a review, see reference 15). Diarrheagenic *E. coli* strains are divided into enterotoxigenic *E. coli* (ETEC), enteroaggregative *E. coli*, enteroinvasive *E. coli*, diffusely adhering *E. coli*, enteropathogenic *E. coli* (EPEC), and enterohemorrhagic *E. coli* (EHEC) strains (15), which have different virulence mechanisms.

Whole-genome sequencing approaches have revealed that *E. coli* has a conserved core of genes common to both commensal and pathogenic strains. The conserved genome framework is decorated with genomic islands and small clusters of genes that have been acquired by horizontal gene transfer and that in pathogenic strains are often associated with virulence (for a review, see reference 32). EPEC strains provide a striking example of a pathovar highly adapted to virulence in the human intestine (8, 15), but until now no EPEC strain has been fully sequenced.

EPEC was the first pathovar of *E. coli* to be implicated in human disease (4) and remains a leading cause of infantile diarrhea in developing countries (for a review, see reference 6). However, because EPEC strains were found not to invade cells or release diffusible toxins, doubts about their pathogenic potential were raised in the 1960s and 1970s. However, induction of diarrhea in human volunteers (21) provided the decisive evidence that EPEC is a true human pathogen. As a result of this study, one of the strains tested, E2348/69 (serotype O127:H6), isolated in Taunton, United Kingdom, in 1969, became the prototype strain used globally to study EPEC biology and disease. Indeed, E2348/69 is probably the most-studied pathogenic *E. coli* strain, and until now it was impossible to place the vast amount of biological data in a genomic context.

Typical EPEC strains, which belong to a limited number of

* Corresponding author. Mailing address: Flowers Building, Imperial College London, London SW7 2AZ, United Kingdom. Phone: 44 20 7954 5253. Fax: 44 20 7594 3069. E-mail: g.frankel@imperial.ac.uk.

† Supplemental material for this article may be found at http://jb.asm.org/.

▽ Published ahead of print on 24 October 2008.

JOURNAL OF BACTERIOLOGY, Jan. 2009, p. 23–31 Vol. 191, No. 1
0021-9193/09/$08.00+0 doi:10.1128/JB.01017-08

MINIREVIEW

Bioinformatics Resources for the Study of Gene Regulation in Bacteria▽

Julio Collado-Vides,[1]* Heladia Salgado,[1] Enrique Morett,[2] Socorro Gama-Castro,[1] Verónica Jiménez-Jacinto,[1] Irma Martínez-Flores,[1] Alejandra Medina-Rivera,[1] Luis Muñiz-Rascado,[1] Martín Peralta-Gil,[1] and Alberto Santos-Zavaleta[1]

Programa de Genómica Computacional, Centro de Ciencias Genómicas, Universidad Nacional Autónoma de México, A.P. 565-A, Cuernavaca, Morelos 62100, México,[1] and Departamento de Ingeniería Celular y Biocatálisis, Instituto de Biotecnología, Universidad Nacional Autónoma de México, A.P. 510-3, Cuernavaca, Morelos 62100, México[2]

Genomics, which has been identified as the science of the century, is dramatically changing the historically weak relationship between experimental and theoretical biology. The addition to the *Journal of Bacteriology* of a section for computational biology marks a turning point in the history of this dialogue. This minireview is focused on the computational biology of gene regulation in bacteria, defined as the extensive use of bioinformatics tools to increase our understanding of the regulation of gene expression.

The study of gene regulation has been radically affected by the elucidation of full-genome DNA sequences and the subsequent development of high-throughput methodologies for deciphering their expression. Before the genomics era, most research was focused on individual biological systems. A large number of our colleagues, contributors to this journal, have devoted much of their academic careers to the understanding of individual regulatory units describing operons, regulators, and promoters and their roles in the physiology of the cell. These contributions have provided fundamental information to support the most recent efforts for the integrative knowledge of the cell that all the genomics sciences are achieving.

Genomics offers for the microbiologist studying gene regulation the opportunity to understand individual systems in the context of the whole cell. These integrative sciences have also changed the landscape of data available for new discoveries in the evolution of gene regulation. The major challenge of the genomics era is dealing with large amounts of data at all molecular levels and being able to generate integrated biological knowledge from the data. Bioinformatics is essential to progress in this direction, as it provides what is necessary to deal with large amounts of data: databases, algorithms to generate genomic answers to standard questions, overviews, and navigation capabilities, as well as statistical methods to perform and validate analyses.

Current knowledge of gene regulation in prokaryotes is quite diverse, from the constantly increasing number of full genome sequences for which very little experimental work has been performed, including the many genomes that cannot yet be grown in the laboratory or the little-studied archaea, to the few highly characterized bacterial genomes, such as those of *Bacillus subtilis* and *Pseudomonas aeruginosa*, with *Escherichia coli* K-12 being by far the best-known bacterium and free-living organism. Figure 1 shows this strongly unequal distribution of knowledge, with the number of publications on gene regulation, as an example, for the different microbial genomes.

The first exhaustive historical set of regulated promoters and their associated transcription factors (TFs) and TF DNA-binding sites (TFBSs) gathered around 120 σ^{70} and σ^{54} promoters of *E. coli* K-12 (16, 29). This information and the experience obtained were the seeds for what is now RegulonDB (http://regulondb.ccg.unam.mx/), the original source of expert curated knowledge on the regulation of transcription initiation and operon organization in *E. coli* K-12. It contains what is currently the major electronically encoded regulatory network for any free-living organism (25). This information is also contained in EcoCyc, the *E. coli* model organism database, with added curated knowledge on metabolism and transport (http://ecocyc.org/). We estimate that currently around 25% of the interactions of the full cellular regulatory network of transcription initiation have been assembled. RegulonDB should not be conceived of as a database, but as an environment for genomic regulatory investigations, linked to bioinformatics tools that facilitate analyses of upstream regions, together with data sets and tools for microarray analyses and, more recently, direct access to full papers supporting its knowledge. We are not only curating up-to-date original papers, but have also initiated "active annotation," to use Jean-Michelle Claverie's terminology, to more precisely experimentally map promoters by using a high-throughput strategy.

This minireview has been organized taking into account the fact that most of the readers of the *Journal of Bacteriology* are experimentalists. We start with a few examples of lessons on gene regulation from bioinformatics, focusing on promoters, their definition and regulation, and operon structure. The second section summarizes how RegulonDB has been useful to experimentalists, as well as its role as the "gold standard" for implementing bioinformatics predictive methods, topological analyses of the network, and models of the cell. The last section offers a compendium of links to bioinformatics resources on gene regulation in bacteria, illustrating their usage with flowcharts associated with questions on the regulation of gene

* Corresponding author. Mailing address: Programa de Genómica Computacional, Centro de Ciencias Genómicas, Universidad Nacional Autónoma de México, A.P. 565-A, Cuernavaca, Morelos 62100, Mexico. Phone: 52 (777) 3139877. Fax: 52 (777) 3175581. E-mail: collado@ccg.unam.mx.

▽ Published ahead of print on 31 October 2008.

JOURNAL OF BACTERIOLOGY, Jan. 2009, p. 428–433 Vol. 191, No. 1
0021-9193/09/$08.00+0 doi:10.1128/JB.01234-08

Transcriptome Divergence and the Loss of Plasticity in *Bacillus subtilis* after 6,000 Generations of Evolution under Relaxed Selection for Sporulation▽†

Heather Maughan,[1]* C. William Birky, Jr.,[1] and Wayne L. Nicholson[2]

Department of Ecology and Evolutionary Biology, University of Arizona, Tucson, Arizona 85721,[1] and Department of Microbiology and Cell Science, University of Florida, Space Life Sciences Laboratory, Kennedy Space Center, Florida 32899[2]

Received 4 September 2008/Accepted 16 October 2008

We used microarrays to identify the causes of sporulation deficiencies in *Bacillus subtilis* after 6,000 generations of evolution. We found that sporulation loss did not result from large-scale deletions; therefore, it must have resulted from smaller indels and/or substitutions. Transcription patterns of one strain versus its ancestor showed that sporulation was not initiated and suggested that sporulation loss may be part of an overall decline in plasticity.

Spore formation by bacteria belonging to the *Firmicutes* is an ecologically beneficial yet energetically costly developmental process; dormant spores can better withstand harsh environmental insults (e.g., heat, desiccation, radiation, and oxidative and chemical attacks [13, 14, 16, 17]) than vegetative cells, but spore formation is costly in that it requires the coordinated transcription of hundreds of genes throughout several hours (reviewed in references 4 and 22 and references therein). Spore formation is a remarkable example of phenotypic plasticity, where cells are able to tailor their gene expression to specific environments or physiological states. In environments where benefits associated with spores are absent and no longer balance the cost of constructing spores, it would be predicted that sporulation ability should be lost over time (for extensive discussion of the theoretical details, see references 7 and 8). In order to test this prediction, we performed a laboratory evolution experiment in which two sets of five *Bacillus subtilis* populations were propagated for 6,000 generations in either the presence (populations 628A through 628E) or the absence (populations 624A through 624E) of strong selection for sporulation (7, 8). We observed that indeed, when *B. subtilis* was evolved without selection for sporulation, the ability to sporulate was either severely reduced (populations 624A and 624C) or completely lost (populations 624B, 624D, and 624E) in the nonsporulating experimental populations (8) (Table 1). It was of interest to know whether sporulation ability was lost because selection favors sporulation mutants in a constant, nutrient-rich environment or whether sporulation had simply become neutral with respect to fitness and mutations in sporulation genes had accumulated over time. These two possibilities were addressed using simulations, which suggested that only one population, 624E, lost sporulation because selection favored its loss (8). Identifying the nature of the selectively advantageous mutation(s) underlying sporulation loss in 624E, and comparing it to the mutation(s) underlying sporulation loss in the other populations, is of interest because such a comparison can facilitate our understanding of why sporulation is adaptive in some natural environments but not in others.

Two types of mutations were examined: large-scale deletions and small-scale changes. Because sporulation is no longer needed in populations 624A to 624E, genome loss via large-scale deletion might occur, in a manner similar to that observed in bacterial endosymbionts evolving in the relatively constant environment of the insect gut (11, 12). Alternatively, small-scale changes (e.g., small insertions/deletions [indels] or single-nucleotide substitutions) in critical sporulation genes could lead to a blockage of sporulation. A long-standing and extensive literature exists documenting the pleiotropic effects of simple mutations in *spo* genes (reviewed in references 4, 21, and 22 and references therein). Furthermore, we have previously shown that the rate of spontaneous mutation to rifampin (rifampicin) resistance increased during evolution in populations 624A to -E by as much as 2 orders of magnitude (7), and many of these mutations were determined to be single-nucleotide changes in *rpoB* (15; H. Maughan and W. L. Nicholson, unpublished data).

To address these two possibilities, we used DNA-DNA microarrays to characterize large-scale changes in genome structure and RNA-DNA (transcription) microarrays to assess small-scale changes leading to alterations in gene expression patterns that have occurred during the loss of sporulation proficiency.

Large-scale deletions. To determine whether large-scale deletions resulted in the loss of sporulation genes, we prepared chromosomal DNA from single colonies isolated from each of populations 624A to 624E, propagated for 6,000 generations under relaxed selective pressure for sporulation, and from each of populations 628A to 628E, propagated for 6,000-generations under strong selective pressure for sporulation. Fluorescently labeled probes generated from the chromosomal DNA of evolved isolates were hybridized to 4,096-open reading frame (ORF) microarray slides prepared from *B. subtilis* strain 168 (Eurogentec, Belgium), along with differentially labeled probes prepared from DNA of the corresponding ancestral strains, WN624 and WN628, respectively. The intensities of each dye were quantified, and

* Corresponding author. Present address: Department of Zoology, University of British Columbia, Vancouver, British Columbia V5Y 2B3, Canada. Phone: (604) 822-6323. Fax: (604) 827-4135. E-mail: maughan@zoology.ubc.ca.

† Supplemental material for this article may be found at http://jb.asm.org/.

▽ Published ahead of print on 24 October 2008.

Novel microchip for *in situ* TEM imaging of living organisms and bio-reactions in aqueous conditions†

Kuo-Liang Liu,[a] Chien-Chen Wu,[b] Ying-Jung Huang,[b] Hwei-Ling Peng,[b] Hwan-You Chang,[c] Pin Chang,[d] Long Hsu[e] and Tri-Rung Yew*[a]

Received 26th March 2008, Accepted 26th June 2008
First published as an Advance Article on the web 12th September 2008
DOI: 10.1039/b804986f

A novel and disposable microchip (K-kit) with SiO_2 nano-membranes was developed and used as a specimen kit for *in situ* imaging of living organisms in an aqueous condition using transmission electron microscopy (TEM) without equipment modification. This K-kit enabled the successful TEM observation of living *Escherichia coli* cells and the tellurite reduction process in *Klebsiella pneumoniae*. The *K. pneumoniae* and *Saccharomyces cerevisiae* can stay alive in K-kit after continuous TEM imaging for up to 14 s and 42 s, respectively. Besides, different tellurite reduction profiles in cells grown in aerobic and anaerobic environments can be clearly revealed. These results demonstrate that the K-kit developed in this paper can be useful for observing living organisms and monitoring biological processes *in situ*.

Introduction

Cellular ultrastructures[1-3] are most commonly examined using transmission electron microscopy (TEM). Although TEM can achieve atomic scale resolution, specimens for TEM observation must be either dry[4-6] or frozen[7-10] due to TEM's high-vacuum operation requirements. Dehydration often causes structural distortion of the sample, and many biological processes cannot be monitored in real time in TEM studies.

Previous studies have attempted to develop environmental TEM for observing wet samples.[11-15] Heide first introduced a specimen chamber (Elmiskop I) to replace conventional TEM sample holders for biological applications.[12] Parsons further modified the specimen chamber by controlling the pressure of various gas and water vapors around the specimen to successfully produce a TEM image of a living human leukocyte.[13] Similar approaches were also applied to observe liquid–solid polymerization reactions[14] and electrochemical metal deposition.[15-17] The similar concept has been successfully developed for imaging liquids, cells, and other wet samples in the scanning electron microscopy by Thiberge *et al.*[18,19] However, it is desirable to develop a disposable specimen kit that can fit in standard TEM sample holders without modification, making high resolution *in situ* imaging of living cells or samples in aqueous solution a powerful tool for many researchers.

To provide an alternative way for living cell imaging in TEM other than environmental TEM that has advantages of controlling various gas and water vapors of specimens, we developed a novel and disposable microchip that functions as a specimen kit, with the advantages of being able to fit into commercially-available TEM and avoiding the contamination of samples of the TEM holder or between samples. This microchip is equipped with SiO_2 nano-membranes that seal living organisms in aqueous condition and shield the subject from the TEM vacuum environment using microelectromechanical system (MEMS) techniques. Using prokaryotic cells such as *Escherichia coli* (*E. coli*) JM109 [pmrkABCD$_{v3}$F][20,21] and *Klebsiella pneumoniae* (*K. pneumoniae*) CG43S3,[22-25] and eukaryotic cells like yeast *Saccharomyces cerevisiae* (*S. cerevisiae*) AH109[26] as examples, we demonstrated in this study the feasibility of this microchip for living organism observation and biological process *in situ* monitoring.

The reasons that we use *K. pneumoniae*, *E. coli*, and *S. cerevisiae* as examples in this study are as follows. *K. pneumoniae* is a ubiquitous bacterium causing many infection in immunocompromised individuals who are hospitalized.[23,27] Heavy metals at specific concentrations form complex compounds to cause a toxic effect in the bacteria, although many genes of bacteria will be involved in maintaining homeostasis of the heavy-metal ion. For example, tellurium compounds have been used as antimicrobial and therapeutic agents.[28] However, an *E. coli* terZABCDE homolog was observed in the large virulence plasmid pLVPK of *K. pneumoniae* CG43S3 and was responsible for tellurite resistance.[23,29,30] *S. cerevisiae*[26] or baker's yeast is the simplest eukaryote and an important model organism.

[a]*Department of Materials Science and Engineering, National Tsing-Hua University, 101, Sec.2, Kuang-Fu Road, Hsinchu, Taiwan 300. E-mail: tryew@mx.nthu.edu.tw; Fax: 886-3-5722366; Tel: 886-936347230*
[b]*Department of Biological Science and Technology, National Chiao-Tung University, 1001, Ta-Hsueh Road, Hsinchu, Taiwan 300*
[c]*Institute of NanoEngineering and MicroSystems, National Tsing-Hua University, 101, Sec.2, Kuang-Fu Road, Hsinchu, Taiwan 300*
[d]*Microsystems Technology Center, ITRI South, Industrial Technology Research Institute, Tainan, Taiwan 709*
[e]*Department of Electrophysics, National Chiao-Tung University, 1001, Ta-Hsueh Road, Hsinchu, Taiwan 300*

† Electronic supplementary information (ESI) available: Fig. S1, fluorescence images of four *K. pneumoniae* samples for pre-TEM, and post-continuous TEM; Fig. S2, fluorescence images of the *K. pneumoniae* pre- and post-accumulated TEM for different durations. See DOI: 10.1039/b804986f

Using ratchets and sorters to fractionate motile cells of *Escherichia coli* by length

S. Elizabeth Hulme,[a] Willow R. DiLuzio,[a,b] Sergey S. Shevkoplyas,[a] Linda Turner,[c] Michael Mayer,[a] Howard C. Berg[c] and George M. Whitesides*[a]

Received 11th June 2008, Accepted 21st August 2008
First published as an Advance Article on the web 1st October 2008
DOI: 10.1039/b809892a

This paper describes the fabrication of a composite agar/PDMS device for enriching short cells in a population of motile *Escherichia coli*. The device incorporated ratcheting microchannels, which directed the motion of swimming cells of *E. coli* through the device, and three sorting junctions, which isolated successively shorter populations of bacteria. The ratcheting microchannels guided cells through the device with an average rate of displacement of (32 ± 9) μm s^{-1}. Within the device, the average length of the cells decreased from 3.8 μm (Coefficient of Variation, CV: 21%) at the entrance, to 3.4 μm (CV: 16%) after the first sorting junction, to 3.2 μm (CV: 19%) after the second sorting junction, to 3.0 μm (CV: 19%) after the third sorting junction.

Introduction

This paper describes a microfabricated device that makes it possible to separate motile cells of *Escherichia coli* by length. The device has two principal components: (i) ratcheting microchannels, which guide cells unidirectionally through the device, and (ii) sorting junctions, which use the turning radius of swimming cells in a microfluidic channel to separate short cells from the population. We believe this ability to isolate the shortest cells in a population will be useful for producing synchronized populations of bacteria. The device consisted of a thin film (1 mm in thickness) of poly(dimethyl siloxane) (PDMS) embossed with microchannels—fabricated using soft lithography[1]—in conformal contact with an agar surface;[2] channels in the device therefore had a floor of agar and a ceiling and sidewalls of PDMS. The operation of the device relied on the passive hydrodynamic interaction of swimming cells of *E. coli* with the fluid, and walls of the channels, in the device; because swimming bacteria are self-propelled it was not necessary to use external pumping—or any other active, external elements—to drive cells through the device. By coupling three sorting junctions together in a single device, we were able to isolate a fraction of short cells in which over 90% of cells had lengths that were below the average length of cells entering the device. We estimate that each cell took approximately 4.7 min—or 8% of the 60 min generation time[3] of K12-derived *E. coli* at 25 °C—to swim through the three sorting junctions.

Directing *E. coli* with ratcheting microchannels

When motile cells of *E. coli* swim in an unrestricted, liquid environment, they execute three-dimensional random walks.[4] In the absence of any attractant or repellant cues, the average displacement with time of a population of *E. coli* swimming in a stationary fluid is zero. In order to facilitate the development of microdevices for studying bacteria, it is desirable to develop methods for controlling the direction of motion of a swimming bacterium. Such methods would be useful for directing bacteria through devices and for effecting relatively large-scale, directed displacements of populations of cells.

A small number of researchers have developed techniques for producing unidirectional movement in microorganisms. Uyeda and coworkers have demonstrated the use of microfabricated tracks to guide the motion of the teardrop-shaped, gliding bacterium *Mycoplasma mobile*.[5] The mechanism for unidirectional guidance in this method was specific to the gliding motility of *M. mobile*. Austin and coworkers developed a one-way gate for swimming *E. coli*.[6] The gate consists of a wall of evenly spaced V-shaped features. Because of the tendency of *E. coli* to swim along walls,[2] cells are funneled though the wall when swimming in one direction, but are diverted away from the wall when swimming in the opposite direction; in this manner, the gate was able to direct swimming *E. coli* from one chamber to another. Based on the same principle—the tendency of *E. coli* to swim along the walls of microfluidic channels—we have developed ratcheting microchannels that direct cells along a defined path, and thus produce a stream of *E. coli* moving in a single direction.

Fractionating *E. coli* by length

The bacterium *E. coli* is a rod-shaped organism, which grows by doubling its length while maintaining a constant width, and then divides symmetrically at its midpoint to reproduce. The resulting daughter cells are one-half the length of the parent cell. As each daughter cell ages and grows, the cycle of lengthening and division repeats.[7–9] Because the length of a bacterium is a measure of its progression through its growth cycle, a method for separating short cells from a population of bacterial cells would

[a]*Department of Chemistry and Chemical Biology, Harvard University, Cambridge, MA, 02138, USA*
[b]*Division of Engineering and Applied Sciences, Harvard University, Cambridge, MA, 02138, USA*
[c]*Rowland Institute at Harvard, Cambridge, MA, 02142, USA*

Incorporation of prefabricated screw, pneumatic, and solenoid valves into microfluidic devices

S. Elizabeth Hulme, Sergey S. Shevkoplyas and George M. Whitesides*

Received 9th June 2008, Accepted 2nd September 2008
First published as an Advance Article on the web 21st October 2008
DOI: 10.1039/b809673b

This paper describes a method for prefabricating screw, pneumatic, and solenoid valves and embedding them in microfluidic devices. This method of prefabrication and embedding is simple, requires no advanced fabrication, and is compatible with soft lithography. Because prefabrication allows many identical valves to be made at one time, the performance across different valves made in the same manner is reproducible. In addition, the performance of a single valve is reproducible over many cycles of opening and closing: an embedded solenoid valve opened and closed a microfluidic channel more than 100,000 times with no apparent deterioration in its function. It was possible to combine all three types of prefabricated valves in a single microfluidic device to control chemical gradients in a microfluidic channel temporally and spatially.

Introduction

This paper demonstrates a technique for creating standardized, prefabricated valves of three types—screw valves, pneumatic valves, and solenoid valves—for microfluidic applications. The valves are fabricated *en masse* before they are needed, and then embedded during the assembly of a microfluidic device. This method of prefabrication and embedding should be useful for introducing both valves, and other functional elements, into microfluidic devices.

As microfluidic technology becomes more sophisticated, there is a growing need for control components—such as valves—that can be integrated easily into microdevices. A variety of microfluidic valves are now available (reviewed in reference[1]), including valves using pneumatic actuation,[2–4] magnetic actuation,[5,6] the swelling of hydrogels,[7] the movement of ferrofluids,[8] and the thermal response of shape-memory alloys.[9] Takayama and coworkers have used the pins of a piezoelectric Braille display as valves in microfluidic systems.[10–15] Most of these valves require sophisticated fabrication or complex controllers, and are therefore not in common use.

Perhaps the most commonly used microfluidic valves in complex elastomeric devices are the pneumatic valves developed by Quake and coworkers.[3] In the Quake valve scheme, each valve is a three-layer microfluidic structure, consisting of a flow channel in one layer separated by a thin elastomeric membrane from a (usually perpendicular) control channel in the layer above. The application of pressurized air (or liquid) to the control channel (with actuation pressures of 5–30 psi, or 35–200 kPa, depending on the sizes of the flow and control channels, and the properties of the elastomeric membrane)[2] closes the flow channel. The Quake valves have made it possible to fabricate a number of complex systems because they are compatible with soft-lithographic technology, because they have a small footprint, and because they can be used in parallel at high densities. They also have two disadvantages: i) the off-chip infrastructure (computer-controlled pneumatic actuators, gas distribution system, computer) required to operate them is costly and bulky, and ii) these valves are "overkill" for simple devices. The Quake valves also share a common disadvantage with most other pneumatic valves: they require a continuing application of pressurized gas to maintain a valve in the "closed" state. Many microfluidic applications may need only one, or a small number, of valves. In these cases, inclusion of even a single Quake valve into the design requires the same three layers of microfabrication as do the much more complex systems for which these valves are best suited; this requirement unnecessarily complicates the fabrication of simple systems.

Quake valves are also inflexible in one sense: because the design of the control layer must be compatible with the design of the flow layer, any changes to the design of the flow layer may require changes in the design of the control layer. Similarly, if one needs to change the position of the valves in a device, the control layer may have to be redesigned. Although these steps are not prohibitively time-consuming, they do slow the iterative process of rapid prototyping. In addition, the fabrication of microfluidic systems incorporating any number of Quake valves requires registration of the flow layer and the control layer (although the use of perpendicular flow and control channels makes this process forgiving).

To meet the need for simple, single- or few-valve construction in microfluidic devices fabricated *via* soft lithography, our group developed what we call TWIST valves.[16] To construct a TWIST valve, a small machine screw is introduced directly above a microfluidic channel in a PDMS (elastomeric) device. The TWIST valve works by converting torque into downward compression. Rotation of the screw results in downward motion of the screw and compression of the underlying microfluidic channel; thus rotation closes the channel. Because this process is reversible (counterclockwise rotation of the screw reopens the microfluidic channel), the embedded screw can be used as a microfluidic valve. Because TWIST valves are fabricated individually and can be inserted into microfluidic systems as

Department of Chemistry and Chemical Biology, Harvard University, 12 Oxford St., Cambridge, MA, USA

Incorporation of prefabricated screw, pneumatic, and solenoid valves into microfluidic devices

S. Elizabeth Hulme, Sergey S. Shevkoplyas and George M. Whitesides*

Received 9th June 2008, Accepted 2nd September 2008
First published as an Advance Article on the web 21st October 2008
DOI: 10.1039/b809673b

This paper describes a method for prefabricating screw, pneumatic, and solenoid valves and embedding them in microfluidic devices. This method of prefabrication and embedding is simple, requires no advanced fabrication, and is compatible with soft lithography. Because prefabrication allows many identical valves to be made at one time, the performance across different valves made in the same manner is reproducible. In addition, the performance of a single valve is reproducible over many cycles of opening and closing: an embedded solenoid valve opened and closed a microfluidic channel more than 100,000 times with no apparent deterioration in its function. It was possible to combine all three types of prefabricated valves in a single microfluidic device to control chemical gradients in a microfluidic channel temporally and spatially.

Introduction

This paper demonstrates a technique for creating standardized, prefabricated valves of three types—screw valves, pneumatic valves, and solenoid valves—for microfluidic applications. The valves are fabricated *en masse* before they are needed, and then embedded during the assembly of a microfluidic device. This method of prefabrication and embedding should be useful for introducing both valves, and other functional elements, into microfluidic devices.

As microfluidic technology becomes more sophisticated, there is a growing need for control components—such as valves—that can be integrated easily into microdevices. A variety of microfluidic valves are now available (reviewed in reference[1]), including valves using pneumatic actuation,[2–4] magnetic actuation,[5,6] the swelling of hydrogels,[7] the movement of ferrofluids,[8] and the thermal response of shape-memory alloys.[9] Takayama and coworkers have used the pins of a piezoelectric Braille display as valves in microfluidic systems.[10–15] Most of these valves require sophisticated fabrication or complex controllers, and are therefore not in common use.

Perhaps the most commonly used microfluidic valves in complex elastomeric devices are the pneumatic valves developed by Quake and coworkers.[3] In the Quake valve scheme, each valve is a three-layer microfluidic structure, consisting of a flow channel in one layer separated by a thin elastomeric membrane from a (usually perpendicular) control channel in the layer above. The application of pressurized air (or liquid) to the control channel (with actuation pressures of 5–30 psi, or 35–200 kPa, depending on the sizes of the flow and control channels, and the properties of the elastomeric membrane)[2] closes the flow channel. The Quake valves have made it possible to fabricate a number of complex systems because they are compatible with soft-lithographic technology, because they have a small footprint, and because they can be used in parallel at high densities. They also have two disadvantages: i) the off-chip infrastructure (computer-controlled pneumatic actuators, gas distribution system, computer) required to operate them is costly and bulky, and ii) these valves are "overkill" for simple devices. The Quake valves also share a common disadvantage with most other pneumatic valves: they require a continuing application of pressurized gas to maintain a valve in the "closed" state. Many microfluidic applications may need only one, or a small number, of valves. In these cases, inclusion of even a single Quake valve into the design requires the same three layers of microfabrication as do the much more complex systems for which these valves are best suited; this requirement unnecessarily complicates the fabrication of simple systems.

Quake valves are also inflexible in one sense: because the design of the control layer must be compatible with the design of the flow layer, any changes to the design of the flow layer may require changes in the design of the control layer. Similarly, if one needs to change the position of the valves in a device, the control layer may have to be redesigned. Although these steps are not prohibitively time-consuming, they do slow the iterative process of rapid prototyping. In addition, the fabrication of microfluidic systems incorporating any number of Quake valves requires registration of the flow layer and the control layer (although the use of perpendicular flow and control channels makes this process forgiving).

To meet the need for simple, single- or few-valve construction in microfluidic devices fabricated *via* soft lithography, our group developed what we call TWIST valves.[16] To construct a TWIST valve, a small machine screw is introduced directly above a microfluidic channel in a PDMS (elastomeric) device. The TWIST valve works by converting torque into downward compression. Rotation of the screw results in downward motion of the screw and compression of the underlying microfluidic channel; thus rotation closes the channel. Because this process is reversible (counterclockwise rotation of the screw reopens the microfluidic channel), the embedded screw can be used as a microfluidic valve. Because TWIST valves are fabricated individually and can be inserted into microfluidic systems as

Department of Chemistry and Chemical Biology, Harvard University, 12 Oxford St., Cambridge, MA, USA

Molecular Microbiology (2008) 70(6), 1397–1407

doi:10.1111/j.1365-2958.2008.06486.x
First published online 24 October 2008

Clustering and dynamics of cytochrome *bd*-I complexes in the *Escherichia coli* plasma membrane *in vivo*

Tchern Lenn,[1†] Mark C. Leake[2,3†] and Conrad W. Mullineaux[1*]
[1]*School of Biological and Chemical Sciences, Queen Mary, University of London, Mile End Road, London E1 4NS, UK.*
[2]*Clarendon Laboratory, Department of Physics, University of Oxford, Parks Road, Oxford OX1 3PU, UK.*
[3]*Oxford Centre for Integrative Systems Biology (OCISB), Department of Biochemistry, University of Oxford, South Parks Road, Oxford OX1 3QU, UK.*

Summary

The cytochrome *bd*-I complex of *Escherichia coli* is a respiratory terminal oxidase and an integral component of the cytoplasmic membrane. As with other respiratory components, the organization and dynamics of this complex in living membranes is unknown. We set out to visualize the distribution and dynamics of this complex *in vivo*. By exchanging *cydB* for *cydB–gfpgcn4* on the *E. coli* chromosome, we produced a strain (YTL01) that expresses functional GFP-tagged cytochrome *bd*-I terminal oxidase complexes under wild-type genetic control. We imaged live YTL01 cells using video-rate epifluorescence and total internal reflection fluorescence (TIRF) microscopy in combination with fluorescence recovery after photobleaching (FRAP) and saw mobile spots of GFP fluorescence in plasma membranes. Numbers of GFP molecules per spot were quantified by step-wise photobleaching giving a broad distribution with a mean of ~76, indicating that cytochrome *bd*-I is concentrated in mobile patches in the *E. coli* plasma membrane. We hypothesize that respiration occurs in mobile membrane patches which we call 'respirazones'.

Introduction

Oxidative phosphorylation (OXPHOS) is a multistep membrane process, which is the result of the concerted activities of multiple enzymes. These enzymes have been best characterized in mammalian mitochondria, where they are found in the inner mitochondrial membrane. In prokaryotes, the OXPHOS membrane is usually the plasma membrane. Research on this subject continues to focus mainly on the structure and function of the individual OXPHOS complexes (for review see Rich, 2003) and regulation of expression at the transcriptional level in prokaryotes (for review see Unden and Bongaerts, 1997). Relatively little is known about the supramolecular organization and interactions of OXPHOS complexes in intact bioenergetic membranes. Two contrasting models of organization have been proposed. For a review of the debate, see Lenaz and Genova (2007). The Random Diffusion model proposes that there is no large-scale organization of complexes: they are randomly dispersed and functionally connected mainly by lateral diffusion of small redox carriers. 'Solid-state' models however suggest that electron transport happens within stable supercomplexes of the respiratory proteins. In agreement with this idea, OXPHOS supercomplexes or 'respirasomes' have been isolated from membranes of mammalian, plant and yeast mitochondria and the bacterium *Paracoccus denitrificans* by blue-native polyacrylamide gel electrophoresis (BN-PAGE) (Schägger, 2002). Structures of these supercomplexes have been resolved by single-particle cryo-electron microscopy (Dudkina *et al.*, 2006; Schäfer *et al.*, 2006).

More generally, the traditional Fluid Mosaic Model of biological membranes (Singer and Nicholson, 1972) is being supplanted by the 'Partitioned' or 'Compartmentalized Fluid' model (Engelman, 2005; Kusumi *et al.*, 2005; Marguet *et al.*, 2006). This new membrane paradigm sees non-random distributions of membrane proteins as the norm rather than the exception.

An attractive approach to studying the organization and dynamics of membrane proteins *in vivo* is to use gene fusions to tag proteins with green fluorescent protein (GFP) or variants. Fluorescence microscopy can then be used to observe the behaviour of the protein in the intact membrane. Such an approach has been applied to OXPHOS complexes by Johnson *et al.* (2004). These authors showed that OXPHOS complexes (ATP synthase and succinate dehydrogenase) are heterogeneously distributed in mobile patches in the *Bacillus subtilis* plasma membrane. However, the genes

Accepted 30 September, 2008. *For correspondence. E-mail c.mullineaux@qmul.ac.uk; Tel. (+44) 20 7882 7008; Fax (+44) 20 8983 0973. †These authors contributed equally to the work.

Molecular Microbiology (2008) 70(5), 1062–1075 ■

doi:10.1111/j.1365-2958.2008.06485.x
First published online 22 October 2008

Mechanistic insight into the ribosome biogenesis functions of the ancient protein KsgA

Keith Connolly,[1] Jason P. Rife[2] and Gloria Culver[1]*
[1]*Departments of Biology and of Biochemistry and Biophysics, University of Rochester, Rochester, NY 14627, USA.*
[2]*Department of Medicinal Chemistry and Institute for Structural Biology and Drug Discovery, Virginia Commonwealth University, Richmond, VA 23298, USA.*

Summary

While the general blueprint of ribosome biogenesis is evolutionarily conserved, most details have diverged considerably. A striking exception to this divergence is the universally conserved KsgA/Dim1p enzyme family, which modifies two adjacent adenosines in the terminal helix of small subunit ribosomal RNA (rRNA). While localization of KsgA on 30S subunits [small ribosomal subunits (SSUs)] and genetic interaction data have suggested that KsgA acts as a ribosome biogenesis factor, mechanistic details and a rationale for its extreme conservation are still lacking. To begin to address these questions we have characterized the function of *Escherichia coli* KsgA *in vivo* using both a *ksgA* deletion strain and a methyltransferase-deficient form of this protein. Our data reveal cold sensitivity and altered ribosomal profiles are associated with a Δ*ksgA* genotype in *E. coli*. Our work also indicates that loss of KsgA alters 16S rRNA processing. These findings allow KsgAs role in SSU biogenesis to be integrated into the network of other identified factors. Moreover, a methyltransferase-inactive form of KsgA, which we show to be deleterious to cell growth, profoundly impairs ribosome biogenesis-prompting discussion of KsgA as a possible antimicrobial drug target. These unexpected data suggest that methylation is a second layer of function for KsgA and that its critical role is as a supervisor of biogenesis of SSUs *in vivo*. These new findings and this proposed regulatory role offer a mechanistic explanation for the extreme conservation of the KsgA/Dim1p enzyme family.

Accepted 30 September, 2008. *For correspondence. E-mail gculver@mail.rochester.edu; Tel. (+1) 585 276 3602; Fax (+1) 585 275 2070.

Introduction

Ribosome biogenesis is a fundamental, multistep process in all organisms. Processing of ribosomal RNA (rRNA) from a primary transcript, modification of rRNAs and ribosomal proteins (r-proteins), and association of the r-proteins with rRNA requires a high level of co-ordination as well as a host of additional factors. The fruition of this process is two discrete ribosomal subunits that associate during translation initiation to form the functional ribosome. In general, such a simplified scheme of ribosome biogenesis appears to be representative of the process throughout evolution.

Examination of ribosome biogenesis at the level of nucleotide modification reveals much divergence of the ribosome maturation process between prokaryotes, eukaryotes and archaea. In particular, among all rRNA modifications, only three are conserved throughout all three kingdoms. One is the conversion of U1958 (*Escherichia coli* numbering) to psuedouridine in large ribosomal subunit (LSU) rRNA (Ofengand, 2002). While this modification itself is conserved, the machinery, and therefore the mechanism by which it is accomplished, differs depending on the kingdom and organism (Ofengand, 2002). The other modifications conserved throughout evolution are the dimethylations of two adjacent adenosines [A1518 and A1519 (*E. coli* numbering)] in the universally conserved 3′ terminal helix of the small ribosomal subunit (SSU) rRNA (helix 45; Van Knippenberg *et al.*, 1984; Brimacombe, 1995). These dimethylation modifications, which are present on almost all known ribosomes with the exception of only two organellar instances (Klootwijk *et al.*, 1972; Steege *et al.*, 1982; Van Buul *et al.*, 1984; Noon *et al.*, 1998), are catalysed by the universally conserved Dim1p/KsgA enzyme family. Hence, these two methylations and the enzyme family responsible for them are unparalleled in terms of their representation in SSU biogenesis and present an interesting challenge to uncover the evolutionary and functional significance of this rRNA modification system.

Identification of *ksgA* came following the isolation of *E. coli* strains that were resistant to the aminoglycoside antibiotic kasugamycin due to the lack of methylation of A1518 and A1519 (Sparling, 1970; Helser *et al.*, 1972; Poldermans *et al.*, 1979a). Complementation studies in

Whole-cell 3D STORM reveals interactions between cellular structures with nanometer-scale resolution

Bo Huang[1,2,4], Sara A Jones[2,4], Boerries Brandenburg[1,2] & Xiaowei Zhuang[1–3]

The ability to directly visualize nanoscopic cellular structures and their spatial relationship in all three dimensions will greatly enhance our understanding of molecular processes in cells. Here we demonstrated multicolor three-dimensional (3D) stochastic optical reconstruction microscopy (STORM) as a tool to quantitatively probe cellular structures and their interactions. To facilitate STORM imaging, we generated photoswitchable probes in several distinct colors by covalently linking a photoswitchable cyanine reporter and an activator molecule to assist bioconjugation. We performed 3D localization in conjunction with focal plane scanning and correction for refractive index mismatch to obtain whole-cell images with a spatial resolution of 20–30 nm and 60–70 nm in the lateral and axial dimensions, respectively. Using this approach, we imaged the entire mitochondrial network in fixed monkey kidney BS-C-1 cells, and studied the spatial relationship between mitochondria and microtubules. The 3D STORM images resolved mitochondrial morphologies as well as mitochondria-microtubule contacts that were obscured in conventional fluorescence images.

As a powerful imaging technique for studying cellular processes, fluorescence microscopy allows noninvasive imaging of live samples with molecular specificity. Because of the limited resolution of fluorescence microscopy, however, many biological structures are too small to be observed in detail, prohibiting analyses of molecular interactions within or between these structures. The resolution of light microscopy is classically limited by diffraction to about 200–300 nm in the lateral direction and 500–800 nm in the axial direction; both of these dimensions are substantially larger than the size of many subcellular structures. To overcome this limit, super-resolution optical microscopy approaches have been developed, attaining an order of magnitude improvement in spatial resolution. One category of approaches is based on controlling the spatial pattern of excitation, including stimulated emission depletion (STED) microscopy and its related reversible saturable optical transitions (RESOLFT) technique[1], and saturated structured illumination microscopy (SSIM)[2]. In particular, spatial resolution of about 40–45 nm in three-dimensions has been recently reported using STED[3]. The other approach is based on single-molecule localization of photoswitchable fluorophores, a method independently reported under different names including stochastic optical reconstruction microscopy (STORM)[4], (fluorescence) photoactivation localization microscopy ((f)PALM)[5,6] and other variants[7]. This approach can generate three-dimensional (3D) super-resolution images by localizing both lateral and axial positions of each photoactivated probe. A lateral resolution of 20–30 nm and an axial resolution of 50–60 nm have been reported using astigmatism imaging, allowing the morphology of nanoscopic cellular structures to be resolved[8]. Similar axial resolutions have been subsequently obtained using bifocal plane imaging[9].

Although it is important to resolve the 3D morphology of a biological structure, much of biology is governed by interactions between structures. Co-localization analyses with multicolor imaging have been extensively used to map the likelihood of interaction between two components, but the accuracy of co-localization is inherently limited by the image resolution. Structured illumination microscopy has been recently used to image multiple cellular components with a twofold improvement in 3D resolution compared to conventional fluorescence microscopy[10]. Substantially higher resolution has been realized in multicolor imaging using two-dimensional (2D) and 3D STED[3,11]. Multicolor super-resolution imaging has also been previously implemented using STORM/(f)PALM in two dimensions[12–14]. However, 2D co-localization analyses can be ambiguous considering that biological structures are 3D.

Here we advance STORM/(f)PALM imaging by combining both multicolor and 3D imaging capabilities. To facilitate multicolor imaging, we synthesized probes with distinct colors by covalently linking the photoswitchable cyanine dyes with activator molecules to form a single, functionalized component ready for bioconjugation. To extend beyond previous 3D STORM work on relatively thin samples[8], we combined focal plane scanning with a new treatment for the spherical aberration induced by refractive index mismatch to image substantially thicker samples and to achieve high-resolution whole-cell imaging. Using these new imaging capabilities, we studied the morphology of the mitochondrial network and the spatial relationship between mitochondria and microtubules in mammalian cells.

[1]Howard Hughes Medical Institute, [2]Department of Chemistry and Chemical Biology, and [3]Department of Physics, Harvard University, 12 Oxford St. Cambridge, Massachusetts 02138, USA. [4]These authors contributed equally to this work. Correspondence should be addressed to X.Z. (zhuang@chemistry.harvard.edu).

RECEIVED 29 JULY; ACCEPTED 29 OCTOBER; PUBLISHED ONLINE 23 NOVEMBER 2008; DOI:10.1038/NMETH.1274

Nanoscale imaging of molecular positions and anisotropies

Travis J Gould[1,5], Mudalige S Gunewardene[1,5], Manasa V Gudheti[1], Vladislav V Verkhusha[2], Shu-Rong Yin[3], Julie A Gosse[4] & Samuel T Hess[1]

Knowledge of the orientation of molecules within biological structures is crucial to understanding the mechanisms of cell function. We present a method to image simultaneously the positions and fluorescence anisotropies of large numbers of single molecules with nanometer lateral resolution within a sample. Based on a simple modification of fluorescence photoactivation localization microscopy (FPALM), polarization (P)-FPALM does not compromise speed or sensitivity. We show results for mouse fibroblasts expressing Dendra2-actin or Dendra2-hemagglutinin.

Light microscopy allows noninvasive imaging of multiple species in biological specimens with single-molecule sensitivity, but diffraction normally limits the resolution to ~150–250 nm. As many biological processes occur on smaller length scales, techniques that can image below the diffraction limit and yield single-molecule information are becoming increasingly important.

Recently developed methods can break the diffraction barrier by stimulated emission depletion[1] or by localization of large numbers of single molecules, and achieve effective resolution in the 10–40 nm range[2–4]. In localization-based methods, small subsets of photoactivatable fluorescent molecules are stochastically activated in the sample by illumination with an activation laser. Photoactivated molecules are illuminated by a second laser, imaged and then deactivated, either actively or by spontaneous photobleaching. The process is repeated until data have been acquired on a sufficiently large number of molecules or all possible molecules. Image analysis is then used to measure the position of each molecule and determine its intensity.

Localization-based methods can now image living cells[5,6], three-dimensional specimens[7,8] and multiple species. These methods, however, do not provide information about the orientation and rotational freedom of individual molecules, which can be used to test the degree of interaction between molecules in biological systems. Furthermore, understanding organization and functionality of molecular machines often requires determination of the orientation of molecules within cellular structures and relative to one another. Previous imaging of single molecule anisotropies has relied on near-field methods[9], shape analysis of molecular images obtained by diffraction-limited techniques[10,11] or other methods of imaging relatively sparse distributions of molecules. We set out to augment the capabilities of localization-based microscopy to obtain high-density maps of single-molecule positions and anisotropies.

We present a method for imaging single-molecule polarization anisotropy (a measure of the orientation of the transition dipole moment of a fluorescent molecule) in biological specimens with resolution below the diffraction limit. Our method is based on fluorescence photoactivation localization microscopy (FPALM)[2] with a modified detection path, and we termed it polarization-FPALM (P-FPALM). The addition of a polarizing beam splitter into the detection path allows simultaneous, spatially separate imaging of the emission polarized parallel and perpendicular to a particular axis within the sample. The two detection paths are adjusted to have the same total length from the microscope tube lens. Analysis of the relative intensities of molecules in the two images yields the anisotropy of each localized molecule. Others have implemented a similar approach to study the rotational mobility of individual fluorescent molecules during single-particle tracking experiments[12].

For imaging, we placed the sample on the stage of an inverted microscope with a ×60, 1.2 numerical aperture (NA) water-immersion objective and illuminated it using two lasers: 405 nm activation and 488 nm readout for the photoactivatable green fluorescent protein (PA-GFP)[13] or 405 nm activation and 556 nm readout for the photoswitchable protein Dendra2 (ref. 14), which can be photoactivated from a green-fluorescent form to a red-fluorescent form. We focused the lasers in the objective back-aperture to cause a large area of the sample to be illuminated with an approximately Gaussian profile with linear polarization along the x, x and y directions for the 405, 488 and 556 nm beams, respectively (**Supplementary Figs. 1** and **2** online). Fluorescence detected by the same objective is filtered by the dichroic mirror and interference filters (**Supplementary Table 1** online), focused by the tube lens to form an intermediate image, which is magnified by a telescope consisting of +60 mm and +200 mm achromatic lenses, to result in an overall magnification of ~192 and an effective pixel size in object space of 83.3 nm. The magnified image was detected with an electron-multiplying charge-coupled device (EMCCD) camera at 10–32 frames per second for ~20–600 s (**Supplementary Table 2** online). The use of a water-immersion lens is an

[1]Department of Physics and Astronomy and Institute for Molecular Biophysics, 5709 Bennett Hall, University of Maine, Orono, Maine 04469, USA. [2]Department of Anatomy and Structural Biology, Albert Einstein College of Medicine, 1300 Morris Park Avenue, Bronx, New York 10461, USA. [3]Laboratory for Cellular and Molecular Biophysics, Program in Physical Biology, National Institute of Child Health and Human Development, 10 Center Drive, Bethesda, Maryland 20892, USA. [4]Department of Biochemistry, Microbiology, and Molecular Biology, 5735 Hitchner Hall, University of Maine, Orono, Maine 04469, USA. [5]These authors contributed equally to this work. Correspondence should be addressed to S.T.H. (sam.hess@umit.maine.edu).

RECEIVED 4 JUNE; ACCEPTED 22 OCTOBER; PUBLISHED ONLINE 16 NOVEMBER 2008; DOI:10.1038/NMETH.1271

Human protein factory for converting the transcriptome into an *in vitro*–expressed proteome

Naoki Goshima[1], Yoshifumi Kawamura[1,2], Akiko Fukumoto[1,2], Aya Miura[1,2], Reiko Honma[3], Ryohei Satoh[2], Ai Wakamatsu[1,4,5], Jun-ichi Yamamoto[5], Kouichi Kimura[6], Tetsuo Nishikawa[5,6], Taichi Andoh[2], Yuki Iida[7], Kumiko Ishikawa[2], Emi Ito[3], Naoko Kagawa[2], Chie Kaminaga[2], Kei-ichi Kanehori[7], Bunsei Kawakami[8], Kiyokazu Kenmochi[2], Rie Kimura[2], Miki Kobayashi[9], Toshihiro Kuroita[8], Hisashi Kuwayama[2], Yukio Maruyama[2], Kiyoshi Matsuo[7], Kazuyoshi Minami[2], Mariko Mitsubori[2], Masatoshi Mori[1,2], Riyo Morishita[1], Atsushi Murase[2], Akira Nishikawa[3], Shigemichi Nishikawa[10], Toshihiko Okamoto[2], Noriko Sakagami[2], Yutaka Sakamoto[2], Yukari Sasaki[2], Tomoe Seki[1,2], Saki Sono[2], Akio Sugiyama[2], Tsuyoshi Sumiya[2], Tomoko Takayama[1,2], Yukiko Takayama[7], Hiroyuki Takeda[2], Takushi Togashi[1,2], Kazuhide Yahata[2], Hiroko Yamada[2], Yuka Yanagisawa[3], Yaeta Endo[11], Fumio Imamoto[12], Yasutomo Kisu[1,2], Shigeo Tanaka[2], Takao Isogai[4,5], Jun-ichi Imai[3], Shinya Watanabe[3] & Nobuo Nomura[1]

Appropriate resources and expression technology necessary for human proteomics on a whole-proteome scale are being developed. We prepared a foundation for simple and efficient production of human proteins using the versatile Gateway vector system. We generated 33,275 human Gateway entry clones for protein synthesis, developed mRNA expression protocols for them and improved the wheat germ cell-free protein synthesis system. We applied this protein expression system to the *in vitro* expression of 13,364 human proteins and assessed their biological activity in two functional categories. Of the 75 tested phosphatases, 58 (77%) showed biological activity. Several cytokines containing disulfide bonds were produced in an active form in a nonreducing wheat germ cell-free expression system. We also manufactured protein microarrays by direct printing of unpurified *in vitro*–synthesized proteins and demonstrated their utility. Our 'human protein factory' infrastructure includes the resources and expression technology for *in vitro* proteome research.

Proteomics on a whole-proteome scale by *in vitro* expression, defined here as *in vitro* proteome research (**Fig. 1**), is now becoming more plausible because of the accumulation of both genome sequencing data[1] and cDNA clones[2–8]. By producing many active proteins easily and simultaneously, we can effectively analyze many biological reactions such as enzyme-substrate reactions, protein-protein interactions, protein modifications and processing by peptidases. *In vitro* research has the advantage of being able to handle proteins that exist in a restricted fashion *in vivo*, such as proteins with tissue-specific, stage-specific or intrinsically rare expression. To pursue *in vitro* study effectively, both resources and expression technologies for proteins with very variable characteristics are required. We describe here the production of the 'human protein factory', an infrastructure with the necessary resources and expression technology for *in vitro* proteome research.

RESULTS

Production of Gateway entry clones and destination vectors

To construct the versatile expression system required for a 'human protein factory', we adopted the Gateway technology[9]. We made the Gateway entry clones[9] by recombining the PCR-amplified open reading frame (ORF) of cDNAs with the *attP* sites of the pDONR201 vector (**Supplementary Methods** and **Supplementary Fig. 1** online). To produce the maximum number of Gateway entry clones, we used 21,485 cDNA clones from multiple sources, including 'full-length long Japan' (FLJ) cDNA clones[2–4] (full-length human cDNA sequencing project) and Mammalian Gene Collection (MGC) clones[5] (Mammalian Gene Collection Program) (**Table 1**). We grouped these cDNAs into 14,862 clusters, which

[1]National Institute of Advanced Industrial Science and Technology, 2-42 Aomi, Koto-ku, Tokyo 135-0064, Japan. [2]Japan Biological Informatics Consortium, TIME24 bldg. 10F, 2-45 Aomi, Koto-ku, Tokyo 135-8073, Japan. [3]Department of Clinical Informatics, Tokyo Medical and Dental University, 1-5-45 Yushima, Bunkyo-ku, Tokyo 113-8519, Japan. [4]Graduate School of Pharmaceutical Sciences, The University of Tokyo, 7-3-1 Hongo, Bunkyo-ku, Tokyo 113-0033, Japan. [5]Reverse Proteomics Research Institute, 1532-3 Yana, Kisarazu, Chiba 292-0818, Japan. [6]Life Science Research Laboratory, Central Research Laboratory, Hitachi, Ltd., 1-280 Higashi-koigakubo, Kokubunji, Tokyo 185-8601, Japan. [7]Hitachi Science Systems, Ltd., 1040 Ichige, Hitachinaka, Ibaraki 312-0033, Japan. [8]Toyobo Co., Ltd., Tsuruga Institute of Biotechnology, 10-24 Toyo-cho, Tsuruga, Fukui 914-0047, Japan. [9]Mitsubishi Chemical Group, Science and Technology Research Center Inc., 1000 Kamoshida-cho, Aoba-ku, Yokohama, Kanagawa 227-8502, Japan. [10]Wakenyaku Co., Ltd., Research and Development Div.–Kusatsu Center, 945-1 Tsujide Shimogasa-cho, Kusatsu, Shiga 525-0029, Japan. [11]Department of Applied Chemistry, Ehime University, 3 Bunkyo-cho, Matsuyama, Ehime 790-8577, Japan. [12]Department of Molecular Biology, Research Institute for Microbial Diseases, Osaka University, 3-1 Yamadaoka, Suita, Osaka 565-0871, Japan. Correspondence should be addressed to N.G. (n-goshima@aist.go.jp) or N.N. (nomura.88@aist.go.jp).

RECEIVED 11 AUGUST; ACCEPTED 14 OCTOBER; PUBLISHED ONLINE 23 NOVEMBER 2008; DOI:10.1038/NMETH.1273

nature
structural &
molecular biology

A quantitative model of transcription factor–activated gene expression

Harold D Kim & Erin K O'Shea

A challenge facing biology is to develop quantitative, predictive models of gene regulation. Eukaryotic promoters contain transcription factor binding sites of differing affinity and accessibility, but we understand little about how these variables combine to generate a fine-tuned, quantitative transcriptional response. Here we used the *PHO5* promoter in budding yeast to quantify the relationship between transcription factor input and gene expression output, termed the gene-regulation function (GRF). A model that captures variable interactions between transcription factors, nucleosomes and the promoter faithfully reproduced the observed quantitative changes in the GRF that occur upon altering the affinity of transcription factor binding sites, and implicates nucleosome-modulated accessibility of transcription factor binding sites in increasing the diversity of gene expression profiles. This work establishes a quantitative framework that can be applied to predict GRFs of other eukaryotic genes.

In eukaryotic cells, environmental stimuli commonly lead to activation of transcription factors and alteration of gene expression levels[1]. Many transcription factors control multiple genes, but these genes are often expressed at different time points and levels, thus differing in induction threshold and expression capacity. Because transcription factors bind to specific DNA sequences in the promoter region to help initiate transcription, the variable mode of interaction between transcription factors and the promoter is key to the diversification of gene expression profiles. For example, the interaction between a transcription factor and DNA can be perturbed by either a change in DNA sequence or a change in the accessibility of the DNA by nucleosomes. However, we currently do not understand how such diverse modes of interaction between transcription factors and promoters translate into quantitative gene expression profiles. To explore these issues, we constructed and empirically tested a quantitative model of transcriptional regulation that captures variable interactions between transcription factors and a nucleosomal promoter.

As a model system, we studied expression of *PHO5*, a *Saccharomyces cerevisiae* gene that encodes an acid phosphatase and is controlled by the transcription factor Pho4. The *PHO5* promoter contains two upstream activation sequences (UASs) recognized by Pho4 and four positioned nucleosomes numbered from –4 through –1 (ref. 2). In conditions of high phosphate concentrations, the low-affinity Pho4 binding site (UASp1) in the nucleosome-free region between nucleosomes –2 and –3 is accessible, whereas the high-affinity binding site (UASp2) is occluded by nucleosome –2 and is inaccessible[3,4] (see box in **Fig. 1**). Under phosphate-starvation conditions, chromatin-modifying and -remodeling complexes are recruited to *PHO5* in a Pho4-dependent manner[5–7] and trigger the displacement of nucleosomes[8,9], a prerequisite for recruitment of the general transcription machinery and transcriptional activation[10,11]. For repression of *PHO5*, the TATA binding protein and RNA polymerase II must be displaced, and nucleosomes must be reassembled[12].

We previously observed that the ratio of the expression level of phosphate-responsive genes in intermediate phosphate concentrations to that in the absence of phosphate depends largely on the affinity of the exposed, non-nucleosomal Pho4 binding sites, whereas the absolute expression level in the absence of phosphate depends more on the affinity of nucleosomal sites[4]. These previous results provided an excellent opportunity to investigate how transcription factor binding and chromatin remodeling combine to produce quantitative regulation of *PHO5* expression. In this new study, we separated the transcription factor Pho4 and the *PHO5* promoter from the phosphate-responsive signaling pathway and measured gene expression output of the *PHO5* promoter as a direct function of Pho4 input—the GRF[13–15]. We constructed a quantitative model of gene expression that relates the affinity and accessibility of transcription factor binding sites in the promoter to the induction threshold and maximum level of expression in relative units. The model faithfully recapitulated the experimentally observed quantitative changes in the induction threshold and the maximum level of the GRF upon altering the affinity of Pho4 binding sites. We anticipate that the method and model presented is broadly applicable to other examples of eukaryotic transcriptional regulation.

Howard Hughes Medical Institute, Departments of Molecular and Cellular Biology, and Chemistry and Chemical Biology, Faculty of Arts and Sciences Center for Systems Biology, Harvard University, Northwest Laboratories, 52 Oxford Street, Room 445.40, Cambridge, Massachusetts 02138, USA. Correspondence should be addressed to E.K.O. (erin_oshea@harvard.edu).

Received 9 April; accepted 23 September; published online 12 October 2008; doi:10.1038/nsmb.1500

nature
structural &
molecular biology

Single-RNA counting reveals alternative modes of gene expression in yeast

Daniel Zenklusen, Daniel R Larson & Robert H Singer

Proper execution of transcriptional programs is a key requirement of gene expression regulation, demanding accurate control of timing and amplitude. How precisely the transcription machinery fulfills this task is not known. Using an *in situ* hybridization approach that detects single mRNA molecules, we measured mRNA abundance and transcriptional activity within single *Saccharomyces cerevisiae* cells. We found that expression levels for particular genes are higher than initially reported and can vary substantially among cells. However, variability for most constitutively expressed genes is unexpectedly small. Combining single-transcript measurements with computational modeling indicates that low expression variation is achieved by transcribing genes using single transcription-initiation events that are clearly separated in time, rather than by transcriptional bursts. In contrast, *PDR5*, a gene regulated by the transcription coactivator complex SAGA, is expressed using transcription bursts, resulting in larger variation. These data directly demonstrate the existence of multiple expression modes used to modulate the transcriptome.

Regulation of gene expression occurs on multiple levels, beginning with promoter accessibility[1]. As a key step in gene expression, transcription is probably one of the most complex and tightly regulated processes within the cell, requiring a series of events to occur in a coordinated fashion to initiate mRNA synthesis[2]. Chromatin rearrangement makes promoters accessible for sequence-specific transcription factors that mediate the assembly of coactivators, additional regulatory factors, the basal transcription machinery and finally RNA polymerase II resulting in initiation[2–5]. Once promoter complexes are assembled, the interaction of transcription factors with DNA keeps the gene active, probably by recruiting polymerases to a preassembled transcription complex. The stability of promoter complexes and their assembly efficiency will therefore influence the amplitude of a transcription response[2–7]. Different *trans*-acting factors and promoter elements including the TATA box have been shown to be important to stabilize promoter complexes and allow efficient transcription, for example, by rapid re-initiation on an assembled promoter complex[3,6,8,9].

As is true for most biological processes, the different steps leading to transcription are subject to stochastic fluctuations[10]. A gene will not be expressed identically in two cells, even if they are grown under the same conditions. Such fluctuations should optimally be minimal, because many proteins such as transcription or splicing factors require well-defined concentrations. High-throughput analyses in yeast showed that protein variation for most genes is low[11]. However, in the yeast *Saccharomyces cerevisiae*, most mRNAs are present in low abundance; 80% of the transcriptome, including many essential genes, are expressed at less than two copies per cell[12]. Therefore, high mRNA expression variation would be likely to lead to a situation where many cells are depleted of essential mRNAs, making it difficult to keep protein levels constant. How the cell keeps this variation low is not known.

This question has been difficult to address owing to technical limitations. Classical ensemble methodologies such as northern blots and reverse-transcription PCR (RT-PCR) are unsuitable for the study of single-cell variability. Most single-cell studies have measured gene expression variation using green fluorescent protein (GFP) reporters to monitor the variability of protein concentrations[13,14]. However, by measuring protein concentration, they could only determine the combined result of transcription and translation, not the direct output of transcription since the mRNA itself was not measured. To understand how cells mediate mRNA expression and how this results in expression variation requires single-cell analysis with single-mRNA resolution.

Few studies have used single-molecule techniques to understand gene expression kinetics. Fluorescence *in situ* hybridization (FISH) suggested that genes in mammalian cells are expressed as 'bursts' of transcription: infrequent periods of transcriptional activity that produce many transcripts within a short time[15]. Such transcription bursts were shown to lead to large variability in mRNA numbers[15]. Using different techniques, transcriptional bursting has been described for many genes and has become the prominent model for gene expression[14,16–20]. Transcriptional bursting has also been observed in bacteria, although in this system bursting was much weaker and measured only on an inducible gene[21]. However, bursting with its consequential large mRNA variation does not explain the low-noise characteristics found

Department of Anatomy and Structural Biology, Albert Einstein College of Medicine, 1300 Morris Park Avenue, Bronx, New York 10461, USA. Correspondence should be addressed to R.H.S. (rhsinger@aecom.yu.edu).

Received 30 June; accepted 14 October; published online 16 November 2008; doi:10.1038/nsmb.1514

ARTICLES

Negative feedback that improves information transmission in yeast signalling

Richard C. Yu[1], C. Gustavo Pesce[1], Alejandro Colman-Lerner[1]†, Larry Lok[1]†, David Pincus[1]†, Eduard Serra[1]†, Mark Holl[2]†, Kirsten Benjamin[1]†, Andrew Gordon[1]† & Roger Brent[1]

Haploid *Saccharomyces cerevisiae* yeast cells use a prototypic cell signalling system to transmit information about the extracellular concentration of mating pheromone secreted by potential mating partners. The ability of cells to respond distinguishably to different pheromone concentrations depends on how much information about pheromone concentration the system can transmit. Here we show that the mitogen-activated protein kinase Fus3 mediates fast-acting negative feedback that adjusts the dose response of the downstream system response to match the dose response of receptor-ligand binding. This 'dose–response alignment', defined by a linear relationship between receptor occupancy and downstream response, can improve the fidelity of information transmission by making downstream responses corresponding to different receptor occupancies more distinguishable and reducing amplification of stochastic noise during signal transmission. We also show that one target of the feedback is a previously uncharacterized signal-promoting function of the regulator of G-protein signalling protein Sst2. Our work suggests that negative feedback is a general mechanism used in signalling systems to align dose responses and thereby increase the fidelity of information transmission.

Cells use signalling systems to sense and transmit information about extracellular conditions. Haploid *Saccharomyces cerevisiae* yeast cells use a prototypic, G-protein-coupled-receptor/mitogen-activated protein kinase (MAPK) cascade signalling system, the pheromone response system[1], to sense and transmit information about the concentration of mating pheromone secreted by cells of the opposite mating type (Fig. 1). The more information about pheromone concentration the system can transmit, the better a cell can distinguish between different pheromone concentrations, an essential ability for proper partner choice and mating. For example, a yeast cell ringed by potential mating partners strongly prefers to mate with partners producing the most pheromone[2]. Partner choice involves two processes that require sensing of pheromone concentration. First, a cell grows up the pheromone concentration gradient[3], a process that probably depends on measurement of precise differences in pheromone concentration at different points on the cell surface. Second, after contacting its partner and forming a prezygote, a cell preferentially completes fusion and forms a diploid with a partner that produces high amounts of pheromone[4]. These experiments indicate that it is important for cells to distinguish among different pheromone concentrations at multiple steps during the mating process.

Previous work suggested that optimal transmission of information about pheromone concentration depends on both distinguishable receptor occupancies and distinguishable downstream system responses. Differences in receptor occupancy are clearly important for mating partner choice and discrimination; for example, in the presence of pheromone at a concentration that saturates the receptor, cells lose the ability to discriminate between high-concentration pheromone-secreting partners and low-concentration pheromone-secreting partners[2]. However, distinguishable receptor occupancies are not sufficient for partner discrimination, as hypersensitive cells, in the presence of pheromone at a concentration that does not saturate the receptor but does saturate downstream responses, also lose the ability to discriminate between partners secreting different levels of pheromone[2]. One complementary study of mating projection orientation in spatial gradients of pheromone showed that hypersensitive cells do not orient their mating projections as precisely as wild-type cells, perhaps because in these cells downstream responses were saturated at most points in the gradient[3]. However, even in pheromone gradient concentrations 100-fold lower, at which downstream responses should not have been saturated, hypersensitive cells still oriented their mating projections less precisely than did wild-type cells in higher concentration gradients[3]. These observations suggest that hypersensitive cells are inherently less able to respond distinguishably to different pheromone concentrations (that is, transmit less information about pheromone concentration), even when they are responding to pheromone concentrations that saturate neither receptor nor downstream responses.

Distinguishable responses and dose–response alignment

One characteristic of wild-type cells that we[5] and others[6] have previously found is that, despite the large number of intermediate signalling events in the system, the dose–response curve of receptor occupancy closely aligns with dose–response curves of downstream system responses. For example, we observe 'dose–response alignment' between receptor occupancy and the accumulated amount

[1]Molecular Sciences Institute, 2168 Shattuck Avenue, Berkeley, California 94704, USA. [2]Microscale Life Sciences Center, University of Washington, Seattle, Washington 98195, USA. †Present addresses: Instituto de Fisiología, Biología Molecular y Neurociencias, CONICET and Departamento de Fisiología, Biología Molecular y Celular, Facultad de Ciencias Exactas y Naturales, Universidad de Buenos Aires, Argentina (A.C.-L.); Synopsys, Mountain View, California 94043, USA (L.L.); Department of Cellular and Molecular Pharmacology, University of California, San Francisco, California 94158, USA (D.P.); Centre de Genètica Mèdica i Molecular, Institut d'Investigació Biomèdica de Bellvitge (IDIBELL), Barcelona 08907, Spain (E.S.); Biodesign Institute, Arizona State University, Tempe, Arizona 85387, USA (M.H.); Amyris Biotechnologies, Emeryville, California 94608, USA (K.B.); Physics Department, Brookhaven National Laboratory, Upton, New York 11973, USA (A.G.).

High-resolution statistical mapping reveals gene territories in live yeast

Axel B Berger[1], Ghislain G Cabal[1,7], Emmanuelle Fabre[2], Tarn Duong[3], Henri Buc[4], Ulf Nehrbass[1,7], Jean-Christophe Olivo-Marin[5], Olivier Gadal[1,6] & Christophe Zimmer[3]

The nonrandom positioning of genes inside eukaryotic cell nuclei is implicated in central nuclear functions. However, the spatial organization of the genome remains largely uncharted, owing to limited resolution of optical microscopy, paucity of nuclear landmarks and moderate cell sampling. We developed a computational imaging approach that creates high-resolution probabilistic maps of subnuclear domains occupied by individual loci in budding yeast through automated analysis of thousands of living cells. After validation, we applied the technique to genes involved in galactose metabolism and ribosome biogenesis. We found that genomic loci are confined to 'gene territories' much smaller than the nucleus, which can be remodeled during transcriptional activation, and that the nucleolus is an important landmark for gene positioning. The technique can be used to visualize and quantify territory positions relative to each other and to nuclear landmarks, and should advance studies of nuclear architecture and function.

The spatial organization of the genome inside eukaryotic cell nuclei is not random, and has a central role in transcriptional regulation, DNA repair and replication[1]. Despite many studies, this organization remains poorly understood. Chromosomes 'painted' by fluorescence *in situ* hybridization in fixed vertebrate cells occupy distinct volumes, termed chromosome territories[2], but individual genetic loci can be detected in and out of such territories[3]. Recent analyses of subnuclear locus positions using precise optical measurements had been similarly restricted to fixed cells[4,5]. In the budding yeast *Saccharomyces cerevisiae*, in which the existence of chromosome territories is disputed[6,7], but in which expression studies and endogenous fluorescent tagging are relatively straightforward[8], several microscopy studies could link subnuclear gene location to gene activity[9–14].

Current imaging studies of nuclear organization suffer from important limitations. First, locus positions are generally described only by distance to the nuclear envelope or center, thus reducing compartmentalization to averages in spherical shells and one-dimensional (1D) radial distance histograms, even when images are three-dimensional (3D)[15]. These 1D descriptions do not account for the geometry of interphase yeast nuclei, where chromosome centromeres are anchored via microtubules and kinetochores to the spindle pole body (SPB), a protein structure embedded in the nuclear envelope[16]. This attachment results in a chromosome configuration that violates spherical symmetry[17,18]. Radial analyses also ignore the nucleolus and thus its role in positioning tRNA genes[19] or ribosomal protein genes[20]. Second, optical microscopy studies have a diffraction-limited resolution of at best ~250–500 nm, thus strongly blurring subcompartments inside yeast nuclei (~1 μm radius). Third, for lack of automation, at most a few hundred or tens of nuclei have been analyzed in static or dynamic imaging studies, respectively. However, because of stochastic motions, gene compartmentalization is at best probabilistic and must be assessed statistically from large populations.

On account of these limitations, spatial nuclear organization and hence its regulatory potential are probably strongly underestimated. Here we describe a computational imaging technique that overcomes these obstacles and generates high resolution probabilistic two-dimensional (2D) maps of gene localization from thousands of cells, which allows for accurate dissection of yeast nuclear architecture *in vivo*. Using this technique, we observed spatial segregation of coregulated galactose genes, nucleolar localization of several ribosome biogenesis genes and strong gene compartmentalization within the small yeast nucleus.

RESULTS

Automated localization of genes and nuclear landmarks

To analyze the spatial location of a given locus in a coordinate frame intrinsic to the *S. cerevisiae* nucleus, we determined the 3D position of the locus relative to the nuclear envelope, the nuclear center and

[1]Institut Pasteur, Unité de Biologie Cellulaire du Noyau, Centre National de la Recherche Scientifique, Unité de Recherche Associée 2582, [2]Institut Pasteur, Unité de Génétique Moléculaire des Levures, Centre National de la Recherche Scientifique, Unité de Recherche Associée 2171, [3]Institut Pasteur, Groupe Imagerie et Modélisation, Centre National de la Recherche Scientifique, Unité de Recherche Associée 2582, [4]Institut Pasteur, Département de Biologie Cellulaire et Infections, and [5]Institut Pasteur, Unité d'Analyse d'Images Quantitative, Centre National de la Recherche Scientifique, Unité de Recherche Associée 2582, 25-28 rue du Docteur Roux, 75015 Paris, France. [6]Laboratoire de Biologie Moléculaire des Eucaryotes, Centre National de la Recherche Scientifique, Unité Mixte de Recherche 5099, Université de Toulouse, 118 route de Narbonne, 31000 Toulouse, France. [7]Present addresses: Instituto de Medicina Molecular, Unidade de Malaria, Av. Professor Egas Moniz, 1649-028 Lisboa, Portugal (G.G.C.) and Institut Pasteur Korea, 39-1, Hawolgok-dong, Sungbuk-gu, Seoul 136-791, Korea (U.N.). Correspondence should be addressed to C.Z. (czimmer@pasteur.fr) or O.G. (olivier.gadal@ibcg.biotoul.fr).

RECEIVED 30 JUNE; ACCEPTED 6 OCTOBER; PUBLISHED ONLINE 2 NOVEMBER 2008; DOI:10.1038/NMETH.1266

nature genetics

Regulatory activity revealed by dynamic correlations in gene expression noise

Mary J Dunlop[1], Robert Sidney Cox III[2], Joseph H Levine[1], Richard M Murray[1] & Michael B Elowitz[2–4]

Gene regulatory interactions are context dependent, active in some cellular states but not in others. Stochastic fluctuations, or 'noise', in gene expression propagate through active, but not inactive, regulatory links[1,2]. Thus, correlations in gene expression noise could provide a noninvasive means to probe the activity states of regulatory links. However, global, 'extrinsic', noise sources generate correlations even without direct regulatory links. Here we show that single-cell time-lapse microscopy, by revealing time lags due to regulation, can discriminate between active regulatory connections and extrinsic noise. We demonstrate this principle mathematically, using stochastic modeling, and experimentally, using simple synthetic gene circuits. We then use this approach to analyze dynamic noise correlations in the galactose metabolism genes of *Escherichia coli*. We find that the CRP-GalS-GalE feed-forward loop is inactive in standard conditions but can become active in a GalR mutant. These results show how noise can help analyze the context dependence of regulatory interactions in endogenous gene circuits.

Cells use circuits composed of interacting genes and proteins to implement diverse cellular and developmental programs. A major goal of systems biology is to connect the regulatory architectures of these circuits to the dynamic behavior of individual cells. However, several problems remain. Quantitative information about biochemical parameters is often minimal. In some cases, it may even be unclear in which direction regulation occurs (who regulates whom). And, most critically here, regulatory links that are active in some cellular states may be inactive in the cell type or context being investigated. This can occur for several reasons. In the simplest case, the concentration of a regulatory factor may be outside its effective range (**Fig. 1a**). Transcription factors may also be inactive as a result of post-translational modification or the absence of necessary cofactors[3,4]. Identifying the subset of regulatory links that are active in a given state would simplify analysis of the circuit as a whole[5].

Recent work has shown that gene expression is intrinsically 'noisy'—subject to stochastic fluctuations—causing substantial cell–cell variability[1,2,6–8]. Fluctuations in the concentration of a regulatory protein can cause corresponding fluctuations in the expression of a target only when the regulatory link is active[1,2]. Thus, gene–gene correlations in expression could provide information about the activity state of regulatory connections without explicit perturbation of cellular components.

Such analysis is complicated, however, by the fact that gene expression correlations arise not only from regulation but also from global variations, or 'extrinsic noise', in the overall rate of expression of all genes[2,6]. For example, fluctuating numbers of ribosomes, polymerase components and cell size can affect the expression of many genes in a cell, positively correlating their expression. In practice, the definition of extrinsic noise depends on how the regulatory system is defined[9]. Here we assume that extrinsic noise is global to all measured genes[2,9,10]. In addition, we assume that all genes also fluctuate independently as a result of 'intrinsic noise', or stochasticity, in their own expression. **Figure 1b** illustrates how these opposing effects prevent discrimination between noise and regulation as a source of correlation in static measurements.

Gene regulation occurs with a delay; it takes time for protein concentrations to build up sufficiently to have a regulatory effect on the downstream genes they control (**Fig. 1c**)[11]. The sign of the delay between a fluctuation in regulator concentration and its effect on target protein levels provides information about the causal direction of the link. Note that no such delay occurs for global extrinsic noise, which affects all genes simultaneously. Thus, by following the expression of multiple genes over time in an individual cell, one can decouple extrinsic noise correlations from regulatory correlations. This effect can be analyzed using the temporal cross-correlation function, which describes how well two signals are correlated when one of them is shifted in time relative to the other. Similar approaches have been used to infer connectivity of *in vitro* metabolic networks[12,13]. As experiments in these studies were not conducted in living cells, a prescribed time-varying input was used to perturb the system and it was unnecessary to consider many of the details particular to actual cellular noise sources.

To further understand noise correlations, we implemented a stochastic model of gene regulation[14], incorporating values for biochemical and noise parameters from a previous study[2] (Methods). We simulated expression of a regulatory protein, *A*, which represses a target gene, *B*, and an additional unregulated gene, *C*. With only

[1]Division of Engineering and Applied Science, [2]Division of Biology, [3]Department of Applied Physics and [4]Howard Hughes Medical Institute, California Institute of Technology 1200 E. California Blvd. M/C 114-96 Pasadena, California 91125, USA. Correspondence should be addressed to M.B.E. (melowitz@caltech.edu).

Received 9 June; accepted 23 September; published online 23 November 2008; doi:10.1038/ng.281

Plasmid 61 (2009) 47–51

Contents lists available at ScienceDirect

Plasmid

journal homepage: www.elsevier.com/locate/yplas

Classification of plasmid vectors using replication origin, selection marker and promoter as criteria

Zhijun Wang [a,*], Li Jin [a,b], Zhenghong Yuan [c], Grzegorz Węgrzyn [d], Alicja Węgrzyn [e]

[a] CAS-MPG Partner Institute for Computational Biology, Shanghai Institute for Biological Sciences, Chinese Academy of Sciences, Yueyang Road 320#, Shanghai 200031, PR China
[b] MOE Key Laboratory of Contemporary Anthropology and Center for Evolutionary Biology, School of Life Sciences and Institutes of Biomedical Sciences, Fudan University, Shanghai 200433, PR China
[c] Key Laboratory of Medical Molecular Virology, Shanghai Medical College, Fudan University, Shanghai 200032, PR China
[d] Department of Molecular Biology, University of Gdańsk, Kładki 24, Gdańsk 80-822, Poland
[e] Laboratory of Molecular Biology (affiliated with the University of Gdańsk), Institute of Biochemistry and Biophysics, Polish Academy of Sciences, Gdańsk 80-822, Poland

ARTICLE INFO

Article history:
Received 20 June 2008
Revised 22 August 2008
Available online 15 October 2008

Communicated by Eva Top

Keywords:
Plasmid classification
Promoter
Replication origin
Selection marker

ABSTRACT

Although plasmid DNA vectors have been extensively applied in biotechnology, there is still a lack of standard plasmid vector classification. Here, we propose a classification method for commonly used plasmid vectors. Plasmid vectors were classified into different classes based on their replication origin, selection marker and promoter information. The replication origins of plasmid vectors were classified as: prokaryotic replication origin, eukaryotic replication origin and viral replication origin. Selection markers of plasmid vectors were mainly classified as ampicillin, kanamycin, neomycin, chloramphenicol, gentamycin, tetracycline, erythromycin, streptomycin, vancomycin and spectinomycin resistance gene markers. Promoter sequences were also classified as prokaryotic, eukaryotic and viral promoters. Finally, the nomenclature of common plasmid vectors has three determinants. We believe that the classification of plasmid vectors can provide useful information for researchers employing molecular cloning procedures. A web service of the plasmid classification was established and it is available from http://www.computationalmedicalbiology.org/plasclas.aspx.

1. Introduction

Plasmids are extrachromosomal genetic elements able to replicate autonomously and to be maintained in a host cell (Ebersbach and Gerdes, 2005; Węgrzyn, 2005; Ghosh et al., 2006). These replicons are commonly used as cloning vectors in genetic engineering.

Plasmids had been commonly classified as F plasmids (Kline and Palchaudhuri, 1980; Seelke et al., 1982), colicinogenic (Col) plasmids (Zverev et al., 1984) and R plasmids over 30 years ago (Datta, 1977). Currently, there are several different methods for plasmid classification, for example, based on replication mechanism, plasmids were classified into rolling-circle replicating (RCR) plasmids, theta replicating plasmids, and plasmids that use the strand-displacement mechanism of replication (del Solar et al., 1998; Espinosa et al., 1995). However, this kind of classification provides only a very limited information. Classification based on plasmid incompatibility was developed in the early 1970s (Chabbert et al., 1972; Richards and Datta, 1979; Sagai et al., 1976; Sasakawa et al., 1980) and is based on possibility of stable simultaneous maintenance of two tested plasmids in one host. Introduction of a plasmid into a strain carrying another plasmid is crucial for this classification. The strain is examined for the presence of the introduced plasmid after selection. If the introduced plasmid is eliminated, these two plasmids

* Corresponding author. Fax: +86 21 64183281.
E-mail address: zjwang@picb.ac.cn (Z. Wang).

0147-619X/$ - see front matter © 2008 Elsevier Inc. All rights reserved.
doi:10.1016/j.plasmid.2008.09.003

Kin Discrimination Increases with Genetic Distance in a Social Amoeba

Elizabeth A. Ostrowski[1☯*], Mariko Katoh[2☯], Gad Shaulsky[1,2], David C. Queller[1], Joan E. Strassmann[1]

1 Department of Ecology and Evolutionary Biology, Rice University, Houston, Texas, United States of America, 2 Department of Molecular and Human Genetics, Baylor College of Medicine, Houston, Texas, United States of America

In the social amoeba *Dictyostelium discoideum*, thousands of cells aggregate upon starvation to form a multicellular fruiting body, and approximately 20% of them die to form a stalk that benefits the others. The aggregative nature of multicellular development makes the cells vulnerable to exploitation by cheaters, and the potential for cheating is indeed high. Cells might avoid being victimized if they can discriminate among individuals and avoid those that are genetically different. We tested how widely social amoebae cooperate by mixing isolates from different localities that cover most of their natural range. We show here that different isolates partially exclude one another during aggregation, and there is a positive relationship between the extent of this exclusion and the genetic distance between strains. Our findings demonstrate that *D. discoideum* cells co-aggregate more with genetically similar than dissimilar individuals, suggesting the existence of a mechanism that discerns the degree of genetic similarity between individuals in this social microorganism.

Citation: Ostrowski EA, Katoh M, Shaulsky G, Queller DC, Strassmann JE (2008) Kin discrimination increases with genetic distance in a social amoeba. PLoS Biol 6(11): e287. doi:10.1371/journal.pbio.0060287

Introduction

The ability to recognize and preferentially interact with kin can favor the evolution of altruistic or cooperative traits [1,2]. Microorganisms exhibit complex social behaviors [3–6], but little is known about the genetic and geographic scale of their cooperation [3]. Social traits, in particular, may be prone to the emergence of incompatibilities: selection to avoid potential costs of cooperation, including cheating, may drive rapid evolution at discrimination or other loci and limit cooperation to closely related strains.

The social amoeba *D. discoideum* (formerly known as the cellular slime mold) offers a unique opportunity to examine the relationship between genetic distance and discrimination in a cooperative microbe. It is haploid, and its genome contains numerous microsatellite loci, which permit quantitative estimation of genetic differences between individuals. It has a geographically restricted range and is found primarily in forest soils of eastern North America and East Asia [7]. Upon starvation, unicellular amoebae assemble in groups of approximately 10^4–10^5 cells to form a multicellular aggregate. The aggregate can migrate toward light and heat and eventually develop into a fruiting body composed of a ball of spores held aloft by a rigid cellular stalk. Approximately 70–80% of the cells in the initial aggregate will form spores, whereas 20–30% of the cells will die and form the stalk. Stalk formation is considered to be altruistic, because stalk cells die to benefit the spores by lifting them above the ground, which may increase their chances of dispersal and protect them from hazards in the soil while they sporulate [8–11].

Aggregation in *D. discoideum* can occur between amoebae that are genetically different, and so evolutionary theory predicts selection for cheaters—genotypes that gain the benefit of the stalk while failing to contribute their fair share to its production [12–15]. Indeed, studies of natural isolates have shown that genetically distinct strains of *D. discoideum* can form chimeras in the laboratory that can differ in their allocation to the prespore versus prestalk regions of the slug [8]. Genetic screens to examine cheating behavior in the laboratory strain have also revealed numerous genes that, when disrupted, lead to that mutant's overrepresentation in the spores [16].

The demonstrated ubiquity and ease of social cheating in *D. discoideum* pose a conundrum—what maintains the victims in nature? One possibility is that cheaters have lower fitness than cooperators when not in chimeras. If this is the case, then the fitness advantage gained by cheaters might be reduced or eliminated by mechanisms that lead to the separation of cheaters and cooperators into distinct fruiting bodies [14,17,18]. There are two explanations for how this separation might occur. One possibility is that cheaters and victims rarely interact, because population structure passively leads to the formation of primarily clonal fruiting bodies. Another possibility is that strains segregate from one another before or during multicellular development, a form of kin discrimination. Kin discrimination differs from kin recognition in that the latter term refers to cognitive processes, whereas kin discrimination describes observable behavioral patterns [19–22]. Evidence for kin discrimination is provided by a study in a different species (*D. purpureum*), which showed that cells segregated from non-identical cells during multicellular development, although no cheating was observed

Academic Editor: Nick H. Barton, University of Edinburgh, United Kingdom

Received June 23, 2008; **Accepted** October 10, 2008; **Published** November 25, 2008

Abbreviations: GFP, green fluorescent protein

* To whom correspondence should be addressed. E-mail: ostrowski@rice.edu

☯ These authors contributed equally to this work.

Quantitative single-molecule imaging by confocal laser scanning microscopy

Vladana Vukojević[a,1], Marcus Heidkamp[b], Yu Ming[a], Björn Johansson[a], Lars Terenius[a], and Rudolf Rigler[c,d,1]

[a]Department of Clinical Neuroscience, Karolinska Institutet, 17176 Stockholm, Sweden; [b]Carl Zeiss MicroImaging GmbH, 07745 Jena, Germany; [c]Department of Medical Biochemistry and Biophysics, Karolinska Institutet, 17177 Stockholm, Sweden; and [d]Laboratory of Biomedical Optics, Swiss Federal Institute of Technology, CH-1015 Lausanne, Switzerland

Communicated by Walter J. Gehring, University of Basel, Basel, Switzerland, October 7, 2008 (received for review April 1, 2008)

A new approach to quantitative single-molecule imaging by confocal laser scanning microscopy (CLSM) is presented. It relies on fluorescence intensity distribution to analyze the molecular occurrence statistics captured by digital imaging and enables direct determination of the number of fluorescent molecules and their diffusion rates without resorting to temporal or spatial autocorrelation analyses. Digital images of fluorescent molecules were recorded by using fast scanning and avalanche photodiode detectors. In this way the signal-to-background ratio was significantly improved, enabling direct quantitative imaging by CLSM. The potential of the proposed approach is demonstrated by using standard solutions of fluorescent dyes, fluorescently labeled DNA molecules, quantum dots, and the Enhanced Green Fluorescent Protein in solution and in live cells. The method was verified by using fluorescence correlation spectroscopy. The relevance for biological applications, in particular, for live cell imaging, is discussed.

fluorescence correlation spectroscopy | live cells | sensitivity

Limited sensitivity and spatial resolution impede the usage of fluorescent microscopy for quantitative analysis of low copy numbers of biologically relevant molecules in live cells. Therefore, methodological and instrumental advancements are required. The aim of our work is to explore the benefits of integrating confocal laser scanning microscopy (CLSM) with fluorescence correlation spectroscopy (FCS) (1–4) as a platform for quantitative imaging of the spatiotemporal dynamics of cellular processes in real time.

Fast scanning was suggested as a possible way to increase signal intensity in CLSM (5–8), but has not been systematically pursued. A contributing factor is that for increased scanning speed the number of detected photons becomes lower. With low photon counts, detector properties become increasingly relevant because the internal noise of the detector may considerably limit the quality of the image. Therefore, our first aim was to build an instrument for CLSM imaging with improved detection efficiency. We achieved this by introducing avalanche photodiodes (APDs) as detectors. Compared with the photomultiplier tubes (PMTs), normally used as detectors in conventional CLSM, the APDs are characterized by higher quantum and collection efficiency—≈70% in APDs compared with 15–25% in PMTs; higher gain, faster response time, and lower dark current (6, 9). The considerably improved signal-to-noise ratio that was achieved by the introduction of APDs enabled the implementation of fast scanning. Fast scanning offers additional advantages: increased fluorescence yield by avoiding intersystem crossing, data collection at higher encountering frequency and from independent volumes, further significantly improving the signal-to-background ratio (SBR) in imaging.

We first demonstrate that improved SBRs enabled us to quantify the average number of molecules in the observation volume element by analyzing the image statistics, without resorting to temporal or spatial autocorrelation analyses. Our results, which report on direct quantitative imaging with single-molecule sensitivity by CLSM, were verified by using classical FCS.

We address temporal resolution of fluorescence imaging in the second part of our study. Slow image acquisition is a standard practice, particularly suitable for imaging fixed biological preparations, but becomes a serious limitation when it comes to studying processes in live cells where molecules are in perpetual motion; they are transported from the sites of their synthesis, to the sites of action, and finally to the degradation sites, exhibiting complex spatiotemporal dynamics. To study molecular motility in live cells with single-molecule sensitivity fast imaging routines are a necessity.

Results

Water solutions of organic fluorescent dyes Rhodamine 6G (Rh6G) and Cyanine 5 (Cy5) were used as reference standards. CLSM images were acquired at scanning speeds 0.64–163.8 μs per pixel. Images were collected without averaging, using a 512 × 512-pixel resolution and 70 × 70-nm pixel size. In the digital image pixel intensity is an integer, $i_p = 0, 1, 2\ldots$, and fluorescence intensity associated with it is related to the scanning speed, $I_{i_p}^{\theta} = i_p/\theta$. For a 1-count pixel in the image acquired at the fastest scanning speed, $\theta = 0.64$ μs per pixel, the fluorescence intensity is $I_1^{0.64} = 1.56$ MHz. The corresponding value in the image acquired at the slowest scanning speed, $\theta = 163.8$ μs per pixel, is $I_1^{163.8} = 6.1$ kHz. Statistical methods were used to analyze the image-associated fluorescence intensity distribution. The results of image analysis were compared with FCS measurements, where temporal autocorrelation analysis was performed to evaluate the average number of particles in the observation volume element and determine the lateral diffusion time of the investigated fluorescence reporter.

Fluorescence Gain by Abolishing Intersystem Crossing. The most readily obtained parameter from image analysis that can be compared with FCS measurements is the average fluorescence count rate (Fig. 1*A*). The average fluorescence count rate determined by imaging ($CR_{\text{image}}^{\theta}$) is:

$$CR_{\text{image}}^{\theta} = \sum_{p=1}^{512\times512} \frac{i_p}{512 \times 512 \cdot \theta} = \sum_{i_p=0,\,1,\,2\ldots} \frac{p_{i_p} \cdot i_p}{512 \times 512 \cdot \theta}$$

$$= \sum_{i_p=0,\,1,\,2\ldots} f_{i_p} \cdot I_{i_p}^{\theta}, \qquad [1]$$

Parts of this work were presented at the 9th Carl Zeiss-sponsored workshop on FCS and related methods, December 4–6, 2006, AlbaNova University Center, Stockholm Sweden.

Author contributions: R.R. designed research; V.V. performed research; M.H., Y.M., B.J., and L.T. contributed new reagents/analytic tools; V.V. and R.R. analyzed data; and V.V. and R.R. wrote the paper.

The authors declare no conflict of interest.

[1]To whom correspondence may be addressed. E-mail: vladana.vukojevic@ki.se or rudolf.rigler@epfl.ch.

This article contains supporting information online at www.pnas.org/cgi/content/full/0809250105/DCSupplemental.

www.pnas.org/cgi/doi/10.1073/pnas.0809250105

Modulation of RNA polymerase II subunit composition by ubiquitylation

Anne Daulny, Fuqiang Geng, Masafumi Muratani[1], Jonathan M. Geisinger[2], Simone E. Salghetti, and William P. Tansey[3]

Cold Spring Harbor Laboratory, 1 Bungtown Road, Cold Spring Harbor, NY 11724

Edited by Alexander Varshavsky, California Institute of Technology, Pasadena, CA, and approved October 22, 2008 (received for review September 18, 2008)

Emerging evidence suggests that components of the ubiquitin–proteasome system are involved in the regulation of gene expression. A variety of factors, including transcriptional activators, coactivators, and histones, are controlled by ubiquitylation, but the mechanisms through which this modification can function in transcription are generally unknown. Here, we report that the *Saccharomyces cerevisiae* protein Asr1 is a RING finger ubiquitin-ligase that binds directly to RNA polymerase II via the carboxyl-terminal domain (CTD) of the largest subunit of the enzyme. We show that interaction of Asr1 with the CTD depends on serine-5 phosphorylation within the CTD and results in ubiquitylation of at least 2 subunits of the enzyme, Rpb1 and Rpb2. Ubiquitylation by Asr1 leads to the ejection of the Rpb4/Rpb7 heterodimer from the polymerase complex and is associated with inactivation of polymerase function. Our data demonstrate that ubiquitylation can directly alter the subunit composition of a core component of the transcriptional machinery and provide a paradigm for how ubiquitin can influence gene activity.

transcription | ubiquitin

The correct regulation of gene transcription depends on mechanisms that regulate the formation and dynamics of large multiprotein complexes during various stages of the transcription process. One of the most prominent of these mechanisms is posttranslational protein modification. Phosphorylation is frequently used to promote and stabilize the interaction of various proteins; recruitment of capping and splicing factors to elongating RNA polymerase II (pol II), for example, is signaled by phosphorylation within the carboxyl-terminal domain (CTD) of its largest subunit (1), although modifications such as methylation (2) and acetylation (3) can also influence critical protein–protein interactions. One modification that has received attention in recent years is ubiquitylation, as it has become evident that modification of transcription proteins by ubiquitin (Ub) (4, 5) plays a role in diverse aspects of gene regulation.

Ub is a 76-amino acid protein that is covalently linked to other proteins by the action of an enzymatic cascade, the last step of which is mediated via a Ub-protein ligase (or E3) that recognizes a specific element within the substrate and promotes transfer of Ub to a lysine residue(s) within that protein (6). The utility of ubiquitylation stems from its specificity and its ability to function as either a "classic" modification or as a signal for substrate destruction by the 26S proteasome. By varying the extent of protein ubiquitylation, the type of poly-Ub chains, or the sites of ubiquitylation in the substrate, Ub can act as either a reversible modifier of protein function or an irreversible mechanism for limiting protein levels.

Several recent sets of studies have revealed that ubiquitylation influences multiple steps in the transcription process. Our particular interest has centered on the connection between ubiquitylation of transcriptional activators and the regulation of gene activity, and we and others have proposed that either ubiquitylation or ubiquitylation and destruction (4, 5) are a positive signal for transcriptional activation and may be important for tight regulation of gene activity. A similar "Ub-clock" model has been proposed for transcriptional coactivators (7). In addition to proteolysis, however, there appear to be significant roles for nondestructive ubiquitylation in transcription. Monoubiquitylation of histone H2B, for example, signals methylation of histones H3 and H4 (8). Oligoubiquitylation of the Met-30 transcription factor can regulate its interaction with important transcriptional partners (9). And ubiquitylation can also control recruitment of the mRNA export machinery protein to sites of transcription (10), coordinating transcription with mRNA export. The diversity of the transcriptional processes that are thus far known to be regulated by ubiquitylation suggests that this modification may participate in many stages of transcription.

We are interested in identifying additional ways in which ubiquitylation impacts transcription and in understanding mechanisms through which this modification can function. This interest has led us to study Asr1, a *Saccharomyces cerevisiae* Ub-ligase that binds directly to the pol II CTD and, via ubiquitylation, inactivates the enzyme by ejecting 2 subunits from the pol II complex. These data reveal that the activity of a core component of the transcriptional machinery can be modified by nonproteolytic ubiquitylation, and demonstrate how Ub can change the composition of a large multiprotein complex.

BIOCHEMISTRY

Results

RPC Proteins. The goal of our work was to identify and characterize proteins that directly connect the transcription and Ub systems. To this end, we surveyed the literature for examples of proteins with probable links to both systems. This analysis led us to rA9, a mammalian protein that was identified in a 2-hybrid screen for factors that bind the CTD of Rpb1, the largest subunit of pol II (11). rA9 contains a domain that binds the CTD (CTD-binding domain; CBD), as well as a series of SR repeats, commonly found in splicing factors. Interestingly, we observed that rA9 also contains a RING finger and a PHD domain, both of which are associated with Ub-ligase activity (12, 13). The combination of CTD-binding and potential E3 activities in rA9 suggested to us that it may function as a Ub-ligase within the context of transcription.

To study rA9, we asked whether a related protein is present in the yeast *S. cerevisiae*. Although BLAST searches failed to identify homologous proteins in yeast, we were able to identify sequences with small, but significant, homology to the CBD in a variety of organisms, including fungi (Fig. 1*A*). Within these proteins, the region of CBD homology is located at the carboxyl terminus of the protein, and, remarkably, the majority contain either an amino-terminal RING finger, or a RING/PHD combination [Fig. 1*B* and supporting information (SI) *Methods*]. We refer to proteins with this architecture as RC (RING/CBD) or RPC (RING/PHD/CBD)

Author contributions: A.D., F.G., M.M., and W.P.T. designed research; A.D., F.G., M.M., J.M.G., and S.E.S. performed research; A.D., F.G., M.M., S.E.S., and W.P.T. analyzed data; and A.D., M.M., S.E.S., and W.P.T. wrote the paper.

The authors declare no conflict of interest.

This article is a PNAS Direct Submission.

[1]Present address: Genome Institute of Singapore, 60 Biopolis Street, 02-01, Genome, Singapore.

[2]Present address: Department of Biology, Case Western Reserve University, 10900 Euclid Avenue, Cleveland, OH 44106.

[3]To whom correspondence should be addressed. E-mail: tansey@cshl.edu.

This article contains supporting information online at www.pnas.org/cgi/content/full/0809372105/DCSupplemental.

Extinction and resurrection in gene networks

Daniel Schultz, Aleksandra M. Walczak[1], José N. Onuchic[2], and Peter G. Wolynes

Center for Theoretical Biological Physics, University of California at San Diego, La Jolla, CA 92093-0374

Contributed by José N. Onuchic, October 16, 2008 (sent for review August 12, 2008)

When gene regulatory networks operate in regimes where the number of protein molecules is so small that the molecular species are on the verge of extinction, the death and resurrection of the species greatly modifies the attractor landscape. Deterministic models and the diffusion approximation to the master equation break down at the limits of protein populations in a way very analogous to the breakdown of geometrical optics that occurs at distances <1 wavelength of light from edges. Stable stochastic attractors arise from extinction and resurrection events that are not predicted by the deterministic description. With this view, we explore the attractors of the regular toggle switch and the exclusive switch, focusing on the effects of cooperative binding and the production of protein in bursts. Our arguments suggest that the stability of lysogeny in the λ-phage may be influenced by such extinction phenomena.

cooperativity | regulation | stochasticity

Genetic networks are nonlinear stochastic systems. The genes, single DNA molecules, are regulated by transcription factors, proteins that are themselves products of other genes within the network (1). The dependence of the expression of a gene directly or indirectly on its own products makes gene switches intrinsically nonlinear (2, 3). Additional nonlinearity also can arise from details of promoter architecture such as binding-site overlap or cooperative binding of proteins to the DNA (4). The discreteness of the molecular entities involved makes genetic networks also intrinsically stochastic (5, 6). Individual binding transitions and the events leading to the production and destruction of gene products introduce "shot noise" into the description of genetic networks (7, 8). Shot noise does not simply modify deterministic behavior. Although continuous deterministic descriptions that neglect the noise present in genetic networks give insight into their behavior, molecular discreteness can lead to entirely novel network behaviors (9, 10). The most dramatic of these effects is the possible extinction of molecular species involved in cellular regulation. After a molecular extinction event occurs, other stochastic molecular processes may resurrect such a species, resetting the dynamics. Such extinction and resurrection events cannot be described simply as the perturbative effects of noise on deterministic behavior (11, 12). Behavior of just this sort is seen in the simplest self-activating gene switch and is manifested in the exact analytical solution of the statistical steady state for that system (13). The exact solution yields a bimodal probability distribution for the gene product concentration, whereas deterministic equations (with additive noise) that average over DNA occupancy would show only a single-peaked unimodal distribution for the protein concentration. The extra peak at low protein number is an effect that depends on the unique single-molecule nature of the gene. The unexpected peak disappears when binding/unbinding events are averaged over as in the macroscopic kinetic description. Effects of this nature where binding/unbinding events are discrete also occur when competition for a binding site is important, as in the combinatorial logic of a gene switch (14). In this article, we more closely examine the nature of the stochastic attractors that arise from extinction events coming from the binding/unbinding of proteins to the DNA. We argue they arise from a breakdown of the Langevin noise description or equivalently the diffusion approximation to the master equation that is commonly used (15, 16). Such a description does not correctly describe the system near the boundaries of the allowed protein concentration, i.e., when species can go extinct. This failure is quite analogous to the breakdown of geometrical optics due to diffraction from edges (17). Although we highlight the phenomenon in different versions of the so-called "toggle switch" (18), a simple network that consists of a pair of mutually repressing genes, these molecular discreteness effects also arise in much more complex genetic networks. In our view, the role of extinction and resurrection in multigene networks is likely to be of general importance.

The Toggle Switch

The Toggle Switch is a small network of 2 genes (A and B) in which the 2 gene products mutually repress each other (18–20) (Fig. 1). If A is on, B will be turned off and vice versa. Such simple verbal reasoning would suggest that this system could always show bistability. Deterministic mathematical analysis, on the other hand, argues otherwise. For simplicity, consider the case where both genes have the same binding characteristics and production rates. The deterministic kinetic rate equations for the concentration of proteins a and b are:

$$\frac{da}{dt} = \frac{g_1 + g_0(b^x/X^{eq})}{1 + b^x/X^{eq}} - ka \qquad [1]$$

$$\frac{db}{dt} = \frac{g_1 + g_0(a^x/X^{eq})}{1 + a^x/X^{eq}} - kb \qquad [2]$$

where g_1 and g_0 are the unrepressed and repressed protein synthesis rates respectively, k is the protein degradation rate and X^{eq} is the dissociation constant of the binding of proteins to DNA. The exponent x is the degree of cooperativity in the binding of the gene. $x = 1$ corresponds to a linear repression and the uncooperative binding of monomers, whereas $x = 2$ means that the transcription factors bind cooperatively as dimers. The deterministic description suggests binding cooperativity is essential for the switch to show bistability. For monomer binding ($x = 1$) the kinetic rate equations allow only 1 fixed point: $a = b = \sqrt{X^{eq2}/4 + g_1X^{eq}/k} - X^{eq}/2$, when $g_0 = 0$. The plots of nullclines and flow field for the switches with similar parameters (Fig. 2) show a single steady state for the binding of monomers. But for binding of dimers ($x = 2$) the deterministic toggle switch can have 2 fixed points when X^{eq} is small enough. To achieve this, the repression must be strong enough to avoid a situation where both proteins are expressed in large quantities. The bifurcation

Author contributions: D.S., A.M.W., J.N.O., and P.G.W. designed research; D.S. performed research; D.S. contributed new reagents/analytic tools; D.S. and A.M.W. analyzed data; and D.S., A.M.W., J.N.O., and P.G.W. wrote the paper.

The authors declare no conflict of interest.

[1]Present address: Princeton Center for Theoretical Science, Princeton University, Princeton, NJ 08544.

[2]To whom correspondence should be addressed. E-mail: jonuchic@ucsd.edu.

This article contains supporting information online at www.pnas.org/cgi/content/full/0810366105/DCSupplemental.

Three-state kinetic mechanism for scaffold-mediated signal transduction

Jason W. Locasale*
Department of Biological Engineering, Massachusetts Institute of Technology, 77 Massachusetts Avenue, Cambridge, Massachusetts 02139, USA

(Received 26 June 2008; revised manuscript received 30 August 2008; published 21 November 2008)

Signaling events in eukaryotic cells are often guided by a scaffolding protein. Scaffold proteins assemble multiple proteins into a spatially localized signaling complex and exert numerous physical effects on signaling pathways. To study these effects, we consider a minimal, three-state kinetic model of scaffold-mediated kinase activation. We first introduce and apply a path summation technique to obtain approximate solutions to a single molecule master equation that governs protein kinase activation. We then consider exact numerical solutions. We comment on when this approximation is appropriate and then use this analysis to illustrate the competition of processes occurring at many time scales that are involved in signal transduction in the presence of a scaffold protein. We find that our minimal model captures how scaffold concentration can influence the times over which signaling is distributed in kinase cascades. For a range of scaffold concentrations, scaffolds allow for signaling to be distributed over multiple decades. The findings are consistent with recent experiments and simulation data. These results provide a framework and offer a mechanism for understanding how scaffold proteins can influence the shape of the waiting time distribution of kinase activation and effectively broaden the times over which protein kinases are activated in the course of cell signaling.

DOI: 10.1103/PhysRevE.78.051921 PACS number(s): 87.16.Xa, 87.18.Mp, 87.18.Vf, 82.20.Uv

INTRODUCTION

Cells detect external signals in the form of stresses, growth factors, DNA damage, hormones, among many others, and integrate them to achieve an appropriate biological response [1]. Biochemical modifications in the form of reversible phosphorylations by enzymes known as kinases are detected by proteins to form networks that are used to integrate these signals [2]. These complex networks are comprised of numerous modular structures that allow for many different biological responses. Signal propagation through these networks is often guided by a scaffold protein [3]. Scaffold proteins assemble multiple kinases (that are activated sequentially in a cascade) in close proximity to form signaling complexes. Scaffold proteins are believed to regulate biochemical signaling pathways in a multitude of ways [3–5].

Experiments have suggested that the scaffold proteins have profound effects on regulating signaling dynamics [6–8]. In particular, a key parameter is believed to be the concentration of scaffold proteins. Recent simulation results [9], which elaborated on these findings, showed that one effect that the concentration of scaffold proteins may have is to control the shape of the waiting time distribution of activation. Recent work has shown that the waiting time distribution is closely related to signal duration (e.g., the time over which an active signaling intermediate persists) [9]. Signal duration is known to be an important determinant in many cell decision making processes [10–12] and therefore, a knowledge of how the concentration of scaffold proteins affect this waiting time distribution is important to understand. The waiting time distribution has been used in multiple theoretical contexts [13,14] to study signaling dynamics and has been measured in different experimental contexts in diverse biology systems [15,16].

In this work, we present a minimal model that aims to understand how changes in signaling dynamics manifested through the first passage time statistics are affected solely by changes in scaffold concentration. The purpose of this study is to first construct and then solve a minimal model that aims to capture these desired effects. Many other factors are undoubtedly important in determining how signaling dynamics are regulated in complex biochemical pathways. These factors include but are not limited to feedback control, allosteric regulation by the scaffold, degradation and internalization rates of the complexes along with many others and have been discussed elsewhere [5,17]. Other complexities such as the multiple phosphorylation sites and the processivity and distributivity of the phosphorylation network [18] also affect the dynamics of signal output. Endocytosis and the time scales associated with protein degradation are also important. Our aim is to investigate concentration effects of scaffolds on regulating signaling dynamics which have shown to be important in experiments and simulations.

We present a coarse grained, minimal model that illustrates how the waiting time distribution of protein kinase activation is modified by the presence of different amounts of scaffold protein. The model involves multiple states in which a single protein kinase, situated at the end of a cascade, resides and corresponding transitions between these states are allowed [19]. We analyze the resulting master equation by first introducing an approximate scheme that involves a weighted path summation over the possible trajectories that an individual kinase can take in the course of its transition from an inactive to an active state [20]. We also consider numerical solutions. We find that, consistent with known simulation results, in certain limits the waiting time distribution of activation sharply decays and is effectively characterized by a single exponential whereas in other re-

*Current address: Department of Systems Biology, Harvard Medical School, Boston, MA 02115; jlocasal@bidmc.harvard.edu

Dynamics and evolution of stochastic bistable gene networks with sensing in fluctuating environments

Andre S. Ribeiro*
Computational Systems Biology Research Group, Department of Signal Processing, Tampere University of Technology, Finland and Center for Computational Physics, University of Coimbra, P-3004-516 Coimbra, Portugal
(Received 5 August 2008; revised manuscript received 28 October 2008; published 2 December 2008)

We study how cells can optimize fitness in variable environments by tuning the internal fluctuations of protein expression of a bistable genetic switch. We model cells as bistable toggle switches whose dynamics are governed by a delayed stochastic simulation algorithm. Each state of the toggle switch makes the cell more fit in one of two environmental conditions. Different noise levels in protein expression yield different fitness values for cells in an environment that randomly switches between the two conditions. We compare the behavior of two cell types, one that can sense the environmental condition and one that cannot. In fast changing environments both cell types evolve to be as noisy as possible while maintaining bistability of the toggle switch. In slowly changing environments, evolved nonsensing cells are less noisy while sensing cells evolve the same noise level as in fast changing environments. Sensing removes the need of genotypic changes to adapt to changes in the environment fluctuation rate, providing an evolutionary advantage in unpredictable environments.

DOI: 10.1103/PhysRevE.78.061902 PACS number(s): 87.16.Yc, 05.45.−a, 87.23.Kg, 87.18.Tt

I. INTRODUCTION

Gene expression is inevitably noisy but the noise level can be tuned and, thus, be subject to selection [1–5]. If evolvable, the evolutionary pathway of the noise of a gene's expression is bound to depend on the processes its proteins are involved in. Rather than minimizing or maximizing the noise level, gene networks might evolve specific noise levels adapted to their tasks and thereby, in many cases, to environmental conditions.

Studies suggest that the noise in the expression level of critical genes ought to be minimized since it is detrimental to organismal fitness. Essential genes of yeast and genes involved in circadian oscillators were found to have expression levels with relatively low noise [5,6].

However, noise in gene expression can be beneficial by creating phenotypic diversity in isogenic populations [7], a selective advantage in unpredictable environmental conditions [8]. Importantly, noise-driven genetic mechanisms can evolve [2]. *Bacillus subtilis* has transient and probabilistic differentiation. The noise in the expression level of ComK, a transcription factor that activates the expression of a set of genes necessary for competence, influences the number of cells that uptake DNA [9].

Recently, a *Saccharomyces cerevisiae* strain was engineered that switches between two phenotypes due to noise in gene expression [10]. Each phenotype is more fit to one of two environments. Comparing two populations with different switching rates, fast switchers outgrew slow ones in rapidly changing environments, while the opposite occurs in rarely changing environments, suggesting that it is advantageous for cells to tune noise-driven interphenotype switching rates to the environment switch rate [10]. The cells did not have mechanisms to sense the environment state. When these exist, they should play a key role in survival in fluctuating environments [8].

We investigate how cells can use noise in gene expression and sensing mechanisms of environmental conditions to adapt to noisy two-state environments. We model individual cells, each with a toggle switch (TS), whose dynamics is driven by a delayed stochastic simulation algorithm [11], in a randomly switching two-state environment. Each state of the TS is more fit to one of the two environment states. The environment effects are modeled by subjecting cells to toxins correspondent to the environment state. Each protein of the TS inhibits one of the toxins, mimicking the function of the gene responsible for resistance to tetracycline in *Escherichia coli* K-12 [12].

For comparison and model validation, we study the dynamics and evolution of two types of cells, differing in how the phenotypic switching is regulated. While both cell types have internal noise-driven switching, as in [10], only one of them can bias the switches by sensing the environment ("sensing cells"), i.e., the TS state of these cells is affected by the toxins' amounts, while in the other cell type it is not ("nonsensing cells").

Simulating the cells dynamics in rapidly and slowly switching two-state environments, we address the following questions: can cells increase fitness by tuning the noise level of the TS? How does the capacity to sense and act upon the environment state affect the cells' dynamics and evolutionary pathway? What advantages sensing mechanisms provide that justify its maintenance, even though there are significant energetic costs in doing so?

II. MODEL

Cell populations are simulated at the single cell level. The cell dynamics are driven by a delayed stochastic simulation algorithm (SSA) [11,13] based on the original SSA [14], and

*andre.sanchesribeiro@tut.fi

The impact of relocalization on GC was then tested by monitoring rates of spontaneous Lys+ colony formation. We found sixfold higher GC rates in the presence of either LexA-Nup84 or LexA-Yif1 compared with LexA (Fig. 5D). This was not associated with loss of viability or altered cell division, although the increase in GC conferred by the perinuclear anchor could reflect either increased damage or increased repair.

To resolve this, we asked whether the enhancement of GC achieved by anchoring required the Nup84-Slx5/Slx8 complex. We monitored GC rates with tethered donor loci in *slx8*Δ or *nup84*Δ and found that the increased GC rate conferred by tethering was lost in the mutants (Fig. 5, D and E). One simple interpretation is that the absence of Slx8 or Nup84 attenuates a repair pathway that requires anchorage at or near nuclear pores.

These data support a functional role for the Nup84 complex as a coordinator of SUMO-dependent repair pathways. There is a remarkable selectivity in the recruitment for irreparable DSBs and collapsed replication forks because we score no shift of stalled replication forks or DSBs reparable by HR. This argues for a specific pathway of repair requiring both the Nup84 complex and the Slx5/Slx8 SUMO-dependent ubiquitin ligase. Given the hypersensitivity of *slx5* and *slx8* mutants to HU (*22*, *25*), we propose that this pathway facilitates collapsed replication fork recovery. Although the translocation of damage to the NE does not require Slx5/Slx8, the enhanced rate of repair conferred by pore association does.

A sumoylated protein may accumulate at collapsed forks or irreparable DSBs, requiring Slx5/Slx8 ubiquinylation and proteasomal degradation to enable appropriate repair. The E-MAP data (Fig. 3A) and the fact that Slx5/Slx8 are physically associated with the proteasome (*31*) support this model (Fig. 5F). Furthermore, the presence of the proteasome at the NE (*32*) provides a rationale for the observed relocalization. Lastly, the proteasome is recruited to DSBs (*33*). Thus, we propose that the Slx5/Slx8 pathway involves targeted degradation of a sumoylated protein bound at collapsed forks or resected breaks (Fig. 5F). The relevant targets of Slx5/Slx8 ubiquitination are unknown, but likely candidates based on E-MAP data include Pol32, Rad27, and Srs2 (Fig. 3) (*21*).

References and Notes

1. R. Schneider, R. Grosschedl, *Genes Dev.* **21**, 3027 (2007).
2. A. Akhtar, S. M. Gasser, *Nat. Rev. Genet.* **8**, 507 (2007).
3. P. Therizols *et al.*, *J. Cell Biol.* **172**, 189 (2006).
4. C. B. Bennett *et al.*, *Nat. Genet.* **29**, 426 (2001).
5. S. Loeillet *et al.*, *DNA Repair* **4**, 459 (2005).
6. X. Pan *et al.*, *Cell* **124**, 1069 (2006).
7. B. Palancade *et al.*, *Mol. Biol. Cell* **18**, 2912 (2007).
8. X. Zhao, C. Y. Wu, G. Blobel, *J. Cell Biol.* **167**, 605 (2004).
9. K. Stade *et al.*, *J. Biol. Chem.* **277**, 49554 (2002).
10. Materials and methods are available as supporting material on *Science* Online.
11. S. E. Lee *et al.*, *Cell* **94**, 399 (1998).
12. F. Hediger, A. Taddei, F. R. Neumann, S. M. Gasser, *Methods Enzymol.* **375**, 345 (2004).
13. K. Dubrana, H. van Attikum, F. Hediger, S. M. Gasser, *J. Cell Sci.* **120**, 4209 (2007).
14. P. Heun, T. Laroche, K. Shimada, P. Furrer, S. M. Gasser, *Science* **294**, 2181 (2001).
15. X. H. Wang, J. E. Haber, *PLoS Biol.* **2**, E21 (2004).
16. M. Lisby, U. H. Mortensen, R. Rothstein, *Nat. Cell Biol.* **5**, 572 (2003).
17. J. A. Tercero, J. F. Diffley, *Nature* **412**, 553 (2001).
18. J. A. Cobb *et al.*, *Genes Dev.* **19**, 3055 (2005).
19. V. Doye, R. Wepf, E. C. Hurt, *EMBO J.* **13**, 6062 (1994).
20. M. Schuldiner *et al.*, *Cell* **123**, 507 (2005).
21. S. R. Collins *et al.*, *Nature* **446**, 806 (2007).
22. J. R. Mullen, V. Kaliraman, S. S. Ibrahim, S. J. Brill, *Genetics* **157**, 103 (2001).
23. Y. Xie *et al.*, *J. Biol. Chem.* **282**, 34176 (2007).
24. R. C. Burgess, S. Rahman, M. Lisby, R. Rothstein, X. Zhao, *Mol. Cell. Biol.* **27**, 6153 (2007).
25. C. Zhang, T. M. Roberts, J. Yang, R. Desai, G. W. Brown, *DNA Repair* **5**, 336 (2006).
26. Z. Wang, G. M. Jones, G. Prelich, *Genetics* **172**, 1499 (2006).
27. L. Yang, J. R. Mullen, S. J. Brill, *Nucleic Acids Res.* **34**, 5541 (2006).
28. J. Prudden *et al.*, *EMBO J.* **26**, 4089 (2007).
29. C. Soustelle *et al.*, *Mol. Cell. Biol.* **24**, 5130 (2004).
30. J. A. Freedman, S. Jinks-Robertson, *Genetics* **162**, 15 (2002).
31. S. R. Collins *et al.*, *Mol. Cell. Proteomics* **6**, 439 (2007).
32. C. Enenkel, A. Lehmann, P. M. Kloetzel, *Mol. Biol. Rep.* **26**, 131 (1999).
33. N. Krogan *et al.*, *Mol. Cell* **16**, 1027 (2004).

34. We thank J. E. Haber, M. Lisby, S. Jinks-Robertson, R. Kolodner, and R. Rothstein for generously providing strains; M. Shales for artwork; K. Saeturn and V. Kalck for technical help; and C. J. Ingles, J. E. Haber, and our laboratories for discussions. We acknowledge the Novartis Research Foundation, Swiss Cancer League, Swiss National Science Foundation, Sandler Family Foundation, NIH, National Cancer Institute of Canada, and Canadian Cancer Society for support.

Supporting Online Material

www.sciencemag.org/cgi/content/full/322/5901/597/DC1
Materials and Methods
Figs. S1 to S7
Table S1
References

7 July 2008; accepted 16 September 2008
10.1126/science.1162790

Splicing Factors Facilitate RNAi-Directed Silencing in Fission Yeast

Elizabeth H. Bayne,[1] Manuela Portoso,[1]* Alexander Kagansky,[1] Isabelle C. Kos-Braun,[1] Takeshi Urano,[2] Karl Ekwall,[3] Flavia Alves,[1] Juri Rappsilber,[1] Robin C. Allshire[1]†

Heterochromatin formation at fission yeast centromeres is directed by RNA interference (RNAi). Noncoding transcripts derived from centromeric repeats are processed into small interfering RNAs (siRNAs) that direct the RNA-induced transcriptional silencing (RITS) effector complex to engage centromere transcripts, resulting in recruitment of the histone H3 lysine 9 methyltransferase Clr4, and hence silencing. We have found that defects in specific splicing factors, but not splicing itself, affect the generation of centromeric siRNAs and consequently centromeric heterochromatin integrity. Moreover, splicing factors physically associate with Cid12, a component of the RNAi machinery, and with centromeric chromatin, consistent with a direct role in RNAi. We propose that spliceosomal complexes provide a platform for siRNA generation and hence facilitate effective centromere repeat silencing.

RNA interference (RNAi) and related pathways regulate gene expression at both transcriptional and posttranscriptional levels. In fission yeast (*Schizosaccharomyces pombe*), RNAi directs the formation of heterochromatin (*1*, *2*). Analogous to metazoan centromeres, fission yeast centromeres comprise a kinetochore domain flanked by outer repeat (*otr*) sequences that are assembled in heterochromatin. These *otr* regions are transcribed by RNA polymerase II (Pol II) and give rise to double-stranded RNA that is processed into small interfering RNAs (siRNAs) by Dicer (Dcr1). These siRNAs are loaded into Argonaute (Ago1), a component of the RNA-induced transcriptional silencing (RITS) effector complex (*3*). siRNAs target RITS to cognate nascent transcripts, resulting in recruitment of further factors including the RDRC complex (comprising Rdp1, Cid12, and Hrr1) (*4*), and ultimately Clr4, which methylates histone H3 on Lys^9 (H3K9me2). H3K9me2 is bound by the HP1-related protein Swi6, which in turn recruits cohesin, critical for centromere function (*5*).

To further dissect the mechanism of RNAi-directed chromatin modification, we previously performed a screen that identified mutations at 12 loci termed *csp* (centromere: suppressor of position effect), which at 25°C alleviate silencing of marker genes inserted in the *otr* of centromere 1 (*6*). Several of the *csp* mutants are alleles of known RNAi components (*7*, *8*). The *csp4* and *csp5* mutants are temperature-sensitive (*ts*) lethal alleles. Complementation and sequencing revealed that *csp4* and *csp5* are alleles of *cwf10* and *prp39*, respectively, both of which encode splicing factors. *csp4*, now denoted *cwf10-1*, creates a missense mutation (C323Y) in the guanosine triphosphate–binding domain of Cwf10.

[1]Wellcome Trust Centre for Cell Biology and Institute of Cell Biology, School of Biological Sciences, University of Edinburgh, 6.34 Swann Building, Edinburgh EH9 3JR, UK. [2]Department of Biochemistry, Shimane University Faculty of Medicine, 89-1 Enya-cho, Izumo 693-8501, Japan. [3]Karolinska Institute, Department of Biosciences and Medical Nutrition, University College Sodertorn, Novum 141, 57 Huddinge, Sweden.

*Present address: Institute of Human Genetics, 141 rue de la Cardonille, 34396 Montpellier, France.
†To whom correspondence should be addressed. E-mail: robin.allshire@ed.ac.uk

Structural Insights into a Circadian Oscillator

Carl Hirschie Johnson,[1]* Martin Egli,[2] Phoebe L. Stewart[3]

An endogenous circadian system in cyanobacteria exerts pervasive control over cellular processes, including global gene expression. Indeed, the entire chromosome undergoes daily cycles of topological changes and compaction. The biochemical machinery underlying a circadian oscillator can be reconstituted in vitro with just three cyanobacterial proteins, KaiA, KaiB, and KaiC. These proteins interact to promote conformational changes and phosphorylation events that determine the phase of the in vitro oscillation. The high-resolution structures of these proteins suggest a ratcheting mechanism by which the KaiABC oscillator ticks unidirectionally. This posttranslational oscillator may interact with transcriptional and translational feedback loops to generate the emergent circadian behavior in vivo. The conjunction of structural, biophysical, and biochemical approaches to this system reveals molecular mechanisms of biological timekeeping.

Many biological processes undergo daily (circadian) rhythms that are dictated by self-sustained biochemical oscillators. These circadian clock systems generate a precise period of ~24 hours in constant conditions (constant light and temperature) that is nearly invariant at different temperatures (temperature compensation) (*1*). Circadian clocks also show entrainment to day and night, predominantly mediated by the daily light/dark cycle, so that the endogenous biological clock is phased appropriately to the environmental cycle (*2*). These properties, especially the period's long time constant and temperature compensation, are difficult to explain biochemically. Full understanding of these unusual oscillators will require knowledge of the structures, functions, and interactions of their molecular components.

Pervasive Circadian Rhythms in a Bacterium

We study the components of the biological clock in the prokaryotic cyanobacterium *Synechococcus elongatus*, which programs many processes to conform optimally to the daily cycle, including photosynthesis, nitrogen fixation, and gene expression (*1–3*). Competition assays among different strains of *S. elongatus* rigorously demonstrated that this clock system significantly enhanced the fitness of the cells in rhythmic environments, but not in nonselective constant environments (*3*). The first circadian rhythm measured in *S. elongatus* was that of *psbAI* promoter activity as assayed by a luciferase reporter in populations of cells (*4*). More recently, a tour de force imaging study visualized the rhythm of luminescence from single bacterial cells (Fig. 1, A and B) (*5*). That study also demonstrated that as single cells divide, the daughter cells maintain the circadian phase of the mother cell (Fig. 1B). Therefore, the circadian clock in cyanobacteria is not perturbed by cell division. That result confirmed studies in populations of cells that showed that the circadian clock ticks away with a period of ~24 hours in cells that are dividing with average doubling times of 6 to 10 hours (*6–8*). Conversely, the circadian clock gates cell division so that there are some times of the day/night cycle when the cells grow without dividing (*6*). Therefore, two independent timing circuits coexist in this unicellular bacterium; the circadian pacemaker provides a checkpoint for the cell-division cycle, but there is no feedback of the cell-division timing circuit upon the circadian clock (*8*).

Although it was the *psbAI* promoter that was initially found to be robustly rhythmic in *S. elongatus* (*4*), further investigation of transcriptional control discovered that essentially all promoters were modulated by the circadian clock (*9*). Even a heterologous promoter from *Escherichia coli* is transcribed rhythmically when inserted ectopically into the cyanobacterial chromosome (*10*). Those observations have now been linked with the discovery that the topology of the entire cyanobacterial chromosome is under the control of this circadian program. The *S. elongatus* chromosome undergoes robust oscillations of compaction and decompaction that can be visualized with DNA-binding dyes (Fig. 1C) (*11*). Moreover, the superhelical status of DNA experiences correlative circadian oscillations (Fig. 1D) (*12*). Such large-scale changes in chromosomal structure and torsion are likely to modulate transcriptional rates. It is therefore possible that rhythmic gene-expression patterns are mediated by daily changes in the topology of the chromosome. From this perspective, the cyanobacterial chromosome might be envisioned as an oscillating nucleoid, or "oscilloid," that regulates all promoters—including heterologous promoters—by torsion-sensitive transcription (*12*). Gene expression in cyanobacteria is also regulated in a circadian fashion by the putative transcriptional factor RpaA; rhythmic gene expression is attenuated when the *rpaA* gene is deleted (*2*, *13*). The phosphorylation status of RpaA is regulated by the two-component system kinase SasA, whose phosphorylation is controlled in turn by the KaiABC oscillator that is described in the next paragraph (*13*). These results support an alternative model in which the SasA/RpaA two-component system mediates signals from the KaiABC oscillator to drive genome-wide transcription rhythms. Although the oscilloid and the SasA/RpaA models appear to be mutually exclusive, an analysis of stochastic gene expression in cyanobacteria (*14*) supports regulation both locally (by DNA topology, for example) and comprehensively (by trans factors such as RpaA).

Cogs and Gears: The Kai Proteins

The clockwork mechanism that controls these global rhythms of transcription, chromosomal topology, and cell division is composed of three essential proteins—KaiA, KaiB, and KaiC—which were identified in 1998 (*15*). Their three-dimensional structures, which became available in 2004 (*16–21*), are the only full-length structures of core circadian clock proteins that have been determined. KaiA is a dimer of intertwined monomers, KaiB has a thioredoxin-like fold and forms dimers and tetramers, and KaiC is a "double-doughnut" hexamer (fig. S1). The structure of KaiC revealed a two-domain fold (N-terminal CI and C-terminal CII lobes) in the monomer and six adenosine 5′-triphosphate (ATP) molecules bound between subunits in both the CI and the CII rings (Fig. 2A). ATP binding within CI serves to stabilize the CI ring that forms the hexamer even in the absence of CII domains (*16*). When the three Kai proteins are combined together with ATP in a test tube, a molecular oscillator is reconstituted (Fig. 1E) (*22*). This in vitro oscillator perpetuates a ~24-hour cycle for at least 10 days (*23*), with KaiC alternating between a hypophosphorylated and a hyperphosphorylated state. KaiC is phosphorylated at serine 431 (S431) and threonine 432 (T432) residues in the CII half (*24*, *25*) (Fig. 3, A and B), whereas the CI ring appears devoid of phosphorylation sites. Phosphorylation of CII residues occurs across the subunit-subunit interface, because S431 and T432 are closest to an ATP molecule that is held by the P loop of the adjacent subunit (Fig. 3A).

KaiC is both an autokinase and an autophosphatase (*26–28*) that rhythmically hydrolyzes 15 ATP molecules per subunit during a complete in vitro cycle (*29*). Because only two ATP molecules are needed to phosphorylate S431 and T432, the consumption of the extra ATP molecules may be used to drive conformational changes within KaiC, including monomer exchange (*23*, *30*, *31*). KaiA promotes the formation of the KaiC hyper-

[1]Department of Biological Sciences, Box 35-1634, Vanderbilt University, Nashville, TN 37235–1634, USA. [2]Department of Biochemistry, Vanderbilt University, Nashville, TN 37235–0146, USA. [3]Department of Molecular Physiology and Biophysics, Vanderbilt University, Nashville, TN 37235–0615, USA.

*To whom correspondence should be addressed. E-mail: carl.h.johnson@vanderbilt.edu